ISSN 0965-545X, Polymer Science, Ser. A, 2011, Vol. 53, No. 10, pp. 871–898. © Pleiades Publishing, Ltd., 2011.
2 Original Russian Text © A.L. Volynskii, L.M. Yarysheva, N.F. Bakeev, 2011, published in Vysokomolekulyarnye Soedineniya, Ser. A, 2011, Vol. 53, No. 10, pp. 1683–1713.

Visualization of Deformation-Induced Structural Rearrangements in Amorphous Polymers[1]

2 **A. L. Volynskii, L. M. Yarysheva, and N. F. Bakeev**

Faculty of Chemistry, Moscow State University, Moscow, 119991 Russia
e-mail: volynskii@mail.ru

Abstract—A technique is proposed for decorating amorphous polymers: Before the deformation (shrinkage) of an amorphous polymer, its surface is decorated with a thin metal coating. The subsequent deformation is accompanied by surface structure formation, which makes the processes that occur in the polymer visible. The proposed technique makes it possible to visualize and describe the mechanism of transfer of the polymer from the surface into the bulk and vice versa and to obtain direct information about the direction of the actual local stress. The technique makes it possible to obtain information about the topological heterogeneity of rubber networks, to reveal the features of structural rearrangements that occur during the cold rolling of amorphous polymers, and to describe the phenomenon of self-elongation during annealing of the oriented PET. These microscopic data explain the following features of the structural and mechanical behavior of glassy polymers from a unified viewpoint: stress relaxation in a polymer in the elastic (Hookean) region of the stress–strain curve, an increase in stress in a deformed glassy polymer during its isometric annealing below T_g, the low-temperature shrinkage of a deformed polymer glass in the strain range below its yield point, the storage of internal energy in a deformed glassy polymer in the strain range below the yield point, some anomalies of thermophysical properties, and some other features.

DOI: 10.1134/S0965545X11100129

One of the key problems of the physical chemistry of polymers is the study of their structure–property relationship. In view of the relevance of this problem, basic and applied research into the deformation mechanism of polymers has been conducted for a few decades, as reflected in numerous monographs and handbooks [1–6]. As a result, many fundamental relationships between the structure and properties of polymers were found. This outcome mostly involved direct research methods, such as various techniques of microscopy and X-ray diffraction analysis. The use of these methods is most efficient for the study of the deformation mechanism of crystalline polymers, whereas in the case of amorphous polymers, they provide little information.

Despite obvious progress in revealing the deformation mechanism of polymers, one of the aspects of this problem remains almost unexplored. In general, any deformation of a solid, in particular, a polymer, is accompanied by a change in its surface area. While the volume of a deformed polymer can remain constant [7], its surface area almost always changes; this fact has not yet been taken into account and analyzed. At the same time, a change in the interfacial area of a solid means that the material from its bulk diffuses into the surface as the interfacial area increases and, accordingly, from the surface into the bulk as the interfacial area decreases. The complex of processes that occur at the interfaces of polymers and various polymer systems has obvious fundamental and applied importance [8].

Rehbinder was the first to analyze the deformation and fracture of solids as a surface phenomenon. He proposed that the deformation of a solid is intrinsically a surface phenomenon and studied the effect of interfacial energy on the deformation process. Through the attack of surfactants on solids, he managed to significantly affect the important characteristics of the material, such as strength and tensile strain [9]. The Rehbinder phenomenon is general in nature; it has been verifieded for polymers [10]. However, the process of change in the surface area of a deformed polymer was not experimentally identified and characterized until recently.

The aim of this review is to describe and illustrate the new technique developed for visualizing changes in the interfacial area during deformation and thermal relaxation of oriented polymers.

[1] This work was supported by the Russian Foundation for Basic Research (project nos. 10-03-90028-Bel_a and 11-03-00699-a), the State Program for Support of Leading Scientific Schools (project NSh 4371.2010.3), and State Contract no. 02.740.11.0143.

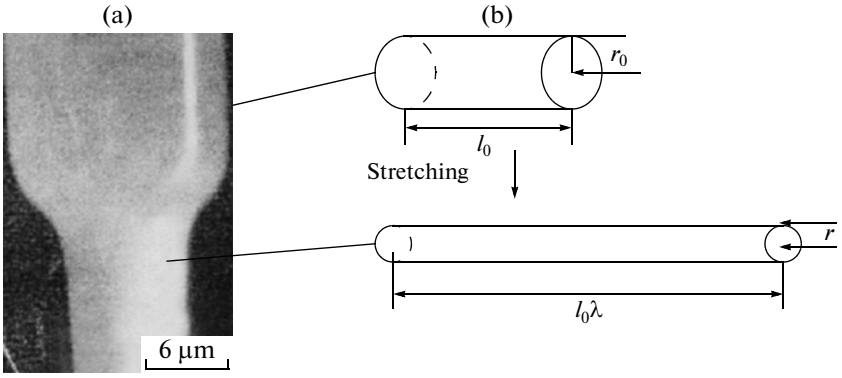

Fig. 1. (a) Micrograph of a polyester fiber in the region of its transition into a neck and (b) diagram of the change in the dimensions of the fiber during its orientation stretching.

TECHNIQUE FOR VISUALIZING STRUCTURAL REARRANGEMENTS THAT OCCUR DURING A CHANGE IN THE SURFACE AREA OF DEFORMED POLYMERS

Change in the Surface Area during Deformation of an Amorphous Polymer

As noted above, a change in the interfacial area occurs after almost any impact on a polymer. Such a change may be characterized mostly via macroscopic measurements of its dimensions. These measurements do not allow observation of the local diffusion of the polymer from its bulk into the surface and vice versa. Figure 1a presents a photograph of the transition region between the original and oriented portions of a PET fiber stretched to necking. It is evident that a significant increase in the surface area of the polymer occurs during the transition of the polymer into a neck.

Consider a cylinder with initial radius r_0 and initial length l_0 (Fig. 1b). For simplicity, assume that the volume of the polymer is preserved during plastic elongation. Let the draw ratio be λ; then, from the volume-conservation condition, we have

$$\pi r_0^2 l_0 = \pi r^2 \lambda l_0 \quad (1)$$

$$r = r_0/\lambda^{-1/2} \quad (2)$$

The surface area of the deformed fiber S is

$$S = 2\pi r \lambda l_0 = S_0 \lambda^{1/2} \quad (3)$$

where S_0 is the initial surface area. Then, moving to the radius of the fiber, we obtain

$$S = S_0(r_0/r), \quad (4)$$

where r_0 and r are the initial and actual radii of the fiber with draw ratio λ.

This relationship unambiguously indicates that a smaller radius of the fiber is associated with a higher specific surface area (i.e., the surface divided by its volume or mass), other things being the same. In the specific case shown in Fig. 1, the surface area of the fiber portion at $l_0 = 1$ cm and $r_0 = 7.5$ μm, which is characteristic of the unstrained fiber (the upper portion of Fig. 1a), is $S_0 = 47.1 \times 10^{-3}$ cm^2. If, however, this fiber is stretched to necking (for polyester, $\lambda \sim 3$), the diameter of the fiber will be $r \sim 3.5$ μm (the lower portion of the fiber in Fig. 1a). Using Eq. (4), we find that the initial surface will increase during cold drawing of the polyester fiber to $S = 100.8 \times 10^{-3}$ cm^2. Thus, the cold drawing of the fiber will lead to an increase in its surface by more than twofold. This means that the polymer undergoes profound rearrangements attributed to migration of the material from the bulk to the surface during its deformation and from the surface into the bulk during the recovery of its dimensions (shrinkage). However, these phenomena are currently not regarded and not taken into account during the study of the deformation mechanism of polymers, primarily because of the lack of an effective research technique.

Deformation is a change in the dimensions of a body under the action of an external force, and shrinkage is a change in the dimensions of a body under the action of an internal stress. A polymer can be deformed in different ways. For example, films and fibers are usually tested under conditions of uniaxial stretching, and bulk samples are tested under uniaxial compression. During the recovery of the original dimensions, the length of deformed fibers and films decreases and the height of the deformed bulk samples increases. Although the signs of these changes are different, in fact, they are representative of the same molecular processes; therefore, the term *shrinkage* is used to describe any process of the recovery of dimensions, regardless of their signs.

Despite a significant increase in the surface area of a polymer during its transition into a neck (the natural draw ratio of PET at room temperature is ~275%), the fiber subjected to this large deformation preserves its smooth cylindrical shape. As a consequence, it is impossible to use a microscopic method to record and characterize the local polymer transport that provides

necking. In accordance with the formulated problem, in this review, we describe a microscopic technique for visualizing changes in the interfacial area during the deformation and thermal relaxation of oriented polymers.

The Physics of the Technique for Visualizing the Structural Rearrangements of Deformed Polymers

Let us consider the theoretical foundations of the proposed method in detail. Electron-microscopic studies of the surface of polymer films with thin hard coatings after their deformation were performed in [11–22]. Figure 2 shows the electron micrographs of the surface relief of polymer films with a thin hard coating after their stretching. The bright bands are fragments of the failed coating, and the dark bands are cracks in it.

The results of simple stretching are that the coating on the polymer surface breaks into many regularly arranged "islands" with approximately the same size and that a regular relief simultaneously appears in it. The regular pattern of the spontaneously occurring relief and its strict orientation relative to the tensile axis are striking. Its valleys and ridges are always oriented strictly parallel to the tensile axis.

The two occurring structures (a regular microrelief and a system of fragments of the failed coating) are highly organized and periodic and can be easily characterized via direct microscopic observations.

Mechanism of formation of a regular microrelief. A question now arises: How does an ordinary polymer film with a coating "organize" this regular structure during simple stretching? Here it is important that a polymer film which is in the rubbery state and subjected to uniaxial stretching simultaneously undergoes two types of deformation. Elongation in one direction is accompanied by contraction (Poisson contraction) in the perpendicular direction. Hence, the hard coating on the surface of the film likewise simultaneously undergoes two types of deformation: compression and extension. This feature of polymers makes it possible to separately consider both the formation of a regular microrelief and the regular fragmentation of the coating that were found in [11–22].

It is the compression of the coating on the polymer surface (Fig. 2) that is responsible for the occurrence of a regular microrelief. This circumstance is of crucial importance for understanding this physical phenomenon.

The coating is an anisodiametric solid tightly bound to the polymer substrate. The processes that accompany the uniaxial compression of anisodiametric solids were first considered by Euler more than 200 years ago. He showed that, during the uniaxial compression of an anisodiametric solid (fiber, film, membrane), after reaching a critical load, the solid loses stability and adopts a half-wave shape (classical Euler buckling instability). If an anisodiametric solid, such as a thin hard coating, is firmly attached to a pliable substrate (base), the pattern of the loss in stability in this coating dramatically changes (Fig. 3). After achievement of the critical compressive load, the solid cannot adopt a half-wave shape, because a deviation from the straight shape would give rise to a restoring

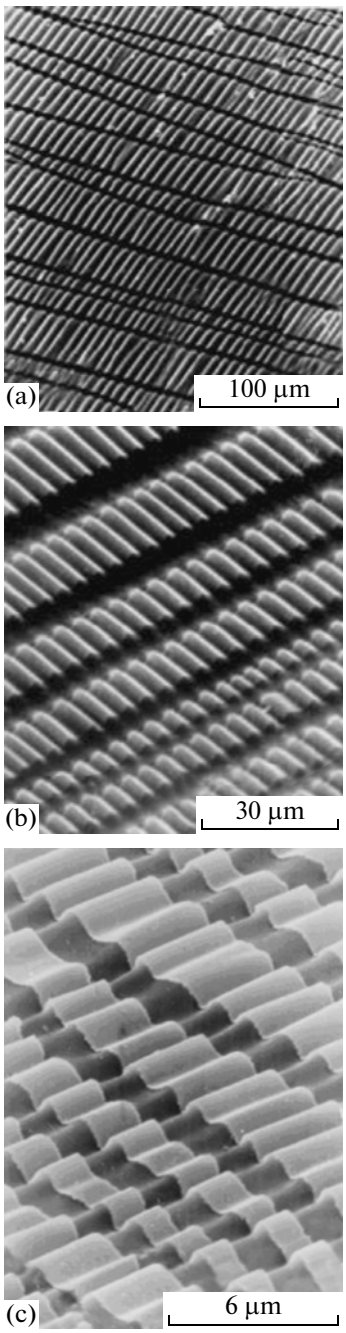

Fig. 2. Scanning electron micrographs of films of (a) natural rubber with a thin (10 nm) gold coating after stretching by 50% at room temperature, (b) PVC with a thin (10 nm) platinum coating, and (c) PET with a thin (15 nm) gold coating after stretching by 100% at 90°C.

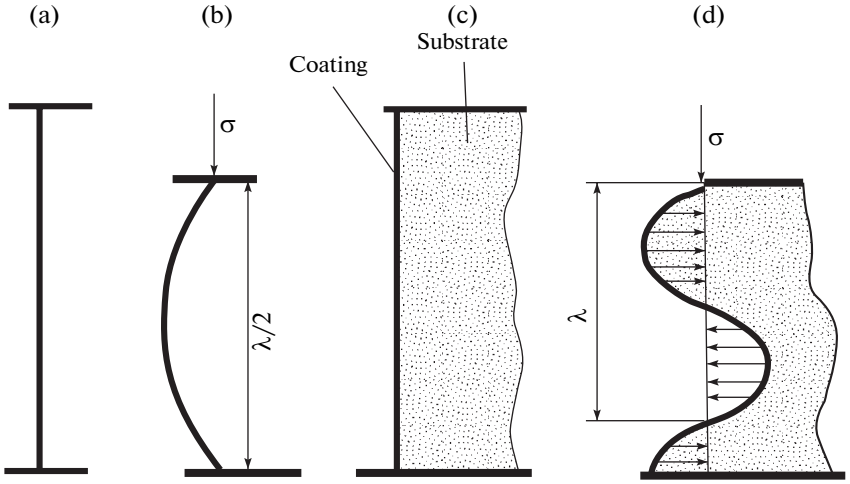

Fig. 3. Diagram of the loss of stability of an asymmetric body (a, b) in a free state and (c, d) on a pliable base.

force from the substrate that is proportional to the value of the deviation. Owing to this interaction between the applied external force and the arising internal resistance from the substrate, the coating will inevitably fold and take a sinusoidal shape with wave period λ. In [11–22], a quantitative relationship between the period of the microrelief, the thickness of the coating, the yield point of the coating, and the stress in the substrate was found. In the context of this review, it is important to note that the occurrence of a regular wavy microrelief is attributed to the compressive deformation of the coating on a pliable substrate.

Regular fragmentation of the coating (Fig. 2) is likewise associated with the transfer of mechanical stress from the deformed polymer to the hard coating tightly bound to it. Regular fragmentation of the coating is not achieved immediately [11–22]. At early stages of stretching, the dimensions of the coating

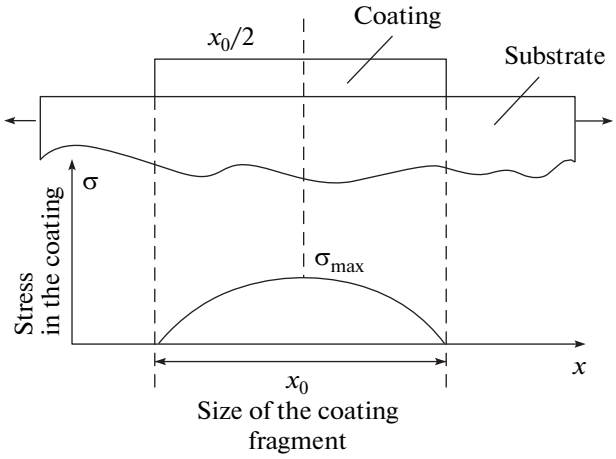

Fig. 4. Diagram of stress distribution in a fragment of a metal coating on the surface deformed via the uniaxial stretching of the polymer substrate.

fragments are not identical. This effect is probably due to the fact that, at the initial stages of failure (at small elongations of the polymer substrate), a decisive contribution to the fragmentation of the coating comes from surface microdefects characteristic of any real solid; they initiate the failure of the coating where they are located. It is evident that these defects are randomly arranged in the coating, a circumstance that causes its irregular random failure. Experimental estimates show that, at the early stages of stretching, the fragment size distribution is very broad.

However, this initial random broad size distribution of coating fragments is followed by a fairly interesting and unique process of further failure of each of the fragments. The fact is that, after the initial fragmentation of the coating, the stretching of the substrate continues; therefore, each resulting fragment remains loaded. The distribution of stress in each fragment is extremely nonuniform (Fig. 4). This stress is zero at the ends of the fragment. With an increase in the distance from the ends, the stress in each fragment increases and achieves its maximum exactly at the center. Further stretching of the substrate is accompanied by an increase in the stress in each fragment and, finally, results in achievement of the ultimate stress. Most importantly, ultimate tensile stress is achieved exactly at the center of the fragment. These processes lead to the amazing process of failure of the coating through its division into two equal parts.

This process can be observed in direct microscopic experiments (Fig. 5). The mechanism of "division" into two equal parts continues as long as the weak pliable substrate can transfer stress that exceeds the ultimate stress of the coating to its fragments. Once the dimensions of all fragments are too small for the substrate to transfer the ultimate tensile stress, the division process is over. In view of this circumstance, the dimensions of the fragments become equal and a sys-

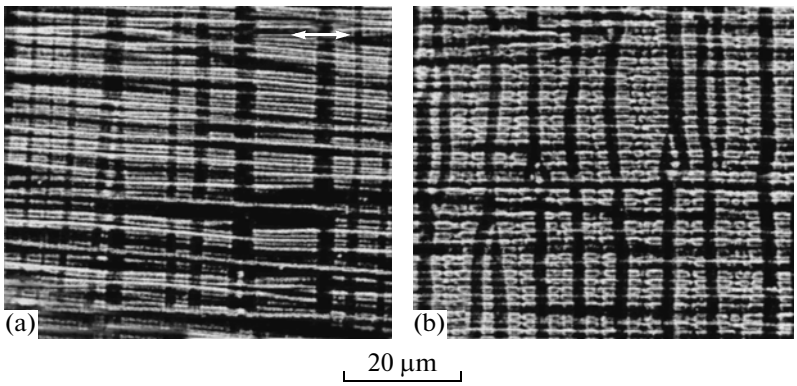

Fig. 5. Scanning electron micrograph of the PET sample with a thin metal coating (a) after its deformation by 50% at 100°C and (b) after further stretching by 50% more at 80°C.

tem of coating fragments with a fairly narrow size distribution is formed on the substrate surface.

Thus, the formation of regular surface structures (wavy relief and size-homogeneous fragments) during deformation of a polymer with a thin hard coating is attributed to the stress that is transferred from the polymer to the coating. The fragmentation of the coating is associated with ultimate tensile stress; the occurrence of a wavy microrelief is related to its uniaxial compression. This simultaneous action leads to the pattern of surface structure formation shown in Fig. 2. Therefore, simple registration of the resulting microrelief makes it possible to not only record the nature of the actual stress (extension or compression) but also determine its direction in an elementary way.

Let us confirm the efficiency of the developed technique in the following experiment. As previously, the metal coating was deposited on the polymer surface via thermal spraying in vacuum. However, a portion of the polymer sample was covered with a screen which was impermeable to the deposited metal. After that, the polymer was subjected to stretching deformation. The region of the polymer on the boundary where the metal was screened is shown in Fig. 6.

It is evident from the micrograph that the boundary is not strict and that the thickness of the deposited layer is gradually thinning away. It is well specified that the above-described structure formation, which is attributed to coating fragmentation and formation of a regular microrelief, occurs in the coating. As the coating becomes thinner, the period of the microrelief and the size of the fragments of the failed coating decrease in full accordance with previously developed concepts [11–22]. The upper right corner of the micrograph depicts the portion of the polymer without the coating. It is clear that this surface has no relief and remains smooth despite deformation. This circumstance means that the diffusion of the polymer from the surface into the bulk and vice versa during deformation of the polymer is not accompanied by the formation of any relief and remains smooth; therefore, the microscopic study of the polymer before and after stretching does not provide information for revealing the deformation mechanism. Thus, Fig. 6 shows the efficiency of the developed technique for visualizing the structural rearrangements of a deformed polymer at providing new information about the internal processes of mass transfer of a polymer during its deformation. Note that it is impossible to retrieve this kind of information by other means.

To conclude this section, one significant factor should be emphasized. It was found that, during deformation of the polymer substrate, the stress responsible for the occurrence of a unique microrelief develops in the deposited coating. In terms of the subject of this review, it is important that this stress is mostly generated by mass-transfer processes in the polymer. In fact,

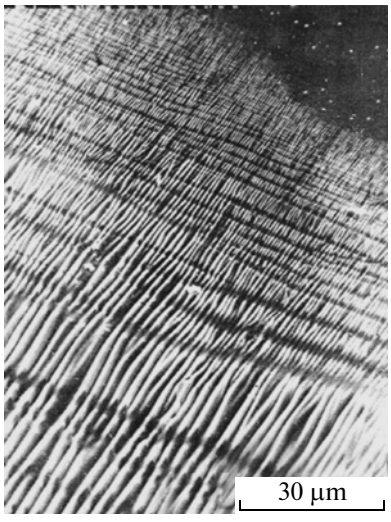

Fig. 6. Scanning electron micrograph of the PET film with a thin (10 nm) layer of copper on the surface that is partially covered with a screen impermeable to the deposited metal (in the upper right corner) after stretching by 100% at 90°C.

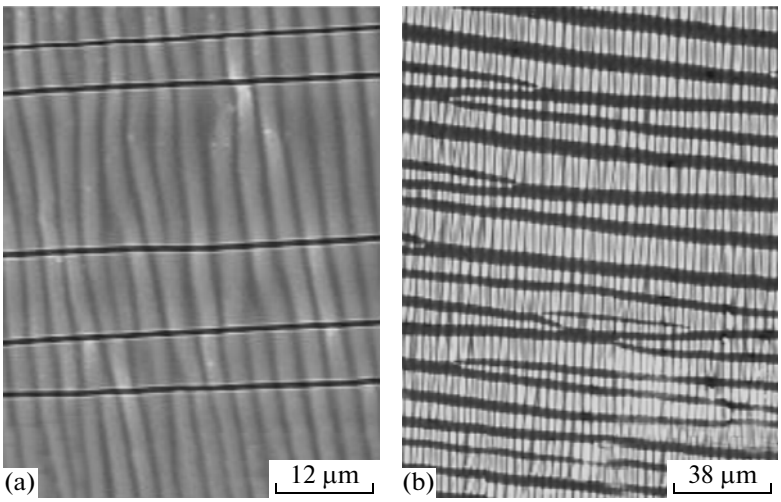

Fig. 7. Scanning electron micrographs of PVC samples with a thin platinum coating stretched by (a) 10 and (b) 100%. The tensile axis is vertical.

as described above, deformation of the polymer is accompanied by migration of the material from the bulk to the surface and vice versa. The coating deposited on the polymer surface is sensitive to these kinds of processes. In the case of a decreasing surface, the coating tightly bound to the polymer cannot migrate into its bulk together with the material of its surface. Consequently, it is under compression and hence loses its stability; according to the described mechanism, a regular microrelief is organized. In the case of stretching of the polymer substrate, the coating tightly bound to the polymer undergoes stretching and then fragments because its tensile strain is less than that of the polymer. All quantitative estimates of surface structure formation are based on the assumption of homogeneity (affinity) of the stress transferred by the substrate to the coating. In this respect, the regular pattern of these structures indirectly suggests the homogeneity of the stress that acts in the polymer.

VISUALIZATION OF STRUCTURAL REARRANGEMENTS THAT ACCOMPANY THE DEFORMATION OF RUBBERY POLYMERS

The investigation of the structural features of the deformation of polymers in the rubbery state holds fundamental and applied importance. However, the problem of obtaining adequate information on the structural rearrangements of rubbery polymers during their deformation remains far from being solved. This is circumstance is primarily due to the fact that rubber networks are amorphous systems that and the use of conventional structural research techniques based on the phase contrast of the studied objects (X-ray diffraction analysis, electron-diffraction study, and microscopy) is inefficient. Therefore, the development of new methods for studying rubbery amorphous polymers is topical.

Uniaxial Deformation

Consider structural rearrangements that occur during the deformation of rubbery polymers with thin metal coatings. The authors of [21] performed a comparative study of two rubbery polymers deformed at room temperature: plasticized PVC ($T_g = -15°C$) and crosslinked synthetic isoprene rubber (SIR). Figure 7 shows typical results of the study of PVC. It is clear that, for small elongations (10%), the metal coating cracks into fragments with approximately the same size (10–30 μm). At the same time, a regular wavy microrelief with a period of ~3 μm is formed on the polymer surface. At this stage of deformation, the microrelief is not yet sufficiently regular. Many of its elements are not clearly pronounced; some originated folds do not extend from one edge of the coating to the other, have a small length, and thin away.

An increase in the strain up to 100% (Fig. 7b) significantly increases the number of cracks in the coating. The size of the fragments of the failure decreases. The deformation of the plasticized PVC samples with a thin metal coating is accompanied by the same types of surface structure formation as in other systems (Fig. 2). Distinct features of this kind of structure formation are the occurrence of a regular microrelief, a regular fragmentation of the coating, and a regular change in the parameters of the microrelief and the dimensions of the coating fragments with an increase in the extension ratio of the polymer-film substrate. The mechanism of these phenomena (the progressive fragmentation of the coating and the change in the microrelief period) is described in greater detail in [15].

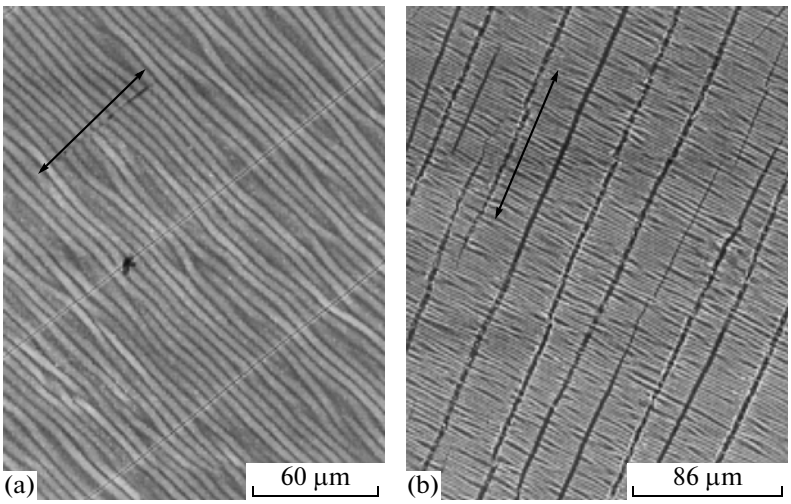

Fig. 8. Scanning electron micrographs of PVC samples that were stretched by (a) 10 and (b) 100%, that were subsequently deposited with a platinum coating, and that were shrunk to the initial state.

The microrelief that is formed on the surface of rubbery polymers can be studied only if the sample dimensions are fixed after deformation. Otherwise, the polymer will completely recover its dimensions and the resulting microrelief will be completely "smooth." Nevertheless, there is a simple and effective method for providing a stable surface microrelief to polymer films in the rubbery state (above T_g). For this purpose, first, it is necessary to stretch the polymer film to the desired elongation ratio; after that, we must fix its dimensions and deposit a thin hard coating on the surface. The subsequent stress release obviously leads to complete shrinkage of the polymer because it is in the rubbery state. During shrinkage, a complete recovery of the geometric dimensions and surface area of the polymer will occur. While this happens, the coating deposited before the shrinkage encounters tensile and compressive stress [15], which will inevitably affect the surface relief. The resulting relief will apparently be stable because the film that underwent complete relaxation after stretching has stable dimensions and a spontaneous change in the surface area cannot occur in it.

The experimental results are shown in Fig. 8. It is clear that the microrelief that occurs on the surface of plasticized PVC during its shrinkage is identical to the relief that results from the "direct" stretching of the polymer (see Fig. 7). In fact, the deformation induces formation of a regular microrelief and a fairly regular fragmentation of the coating (Fig. 8a). As the stretching ratio of the PVC samples increases, the number of cracks in the coating increases and the wavelength of the microrelief decreases (Fig. 8b). However, the relief that results from the shrinkage of the samples of plasticized PVC exhibits one significant difference from the reliefs derived via the direct stretching of this polymer. The entire pattern of this microrelief is turned 90° with respect to the tensile axis in comparison to the relief that occurs during the direct stretching of the polymer samples. This outcome is clear because the polymer film subjected to direct uniaxial stretching simultaneously undergoes two types of deformation. Elongation in one direction is accompanied by contraction in the perpendicular direction. In the case of the shrinkage of a polymer with a coating deposited on its surface, the directions of stretching and subsequent shrinkage are the same; therefore, the entire pattern of structure formation "turns" 90° in comparison to the orientation during direct stretching.

To sum up the above, we can conclude that observations of surface structure formation in a metal coating suggest the equilibrium deformation of plasticized PVC. This is evidenced by the fact that the patterns of surface structure formation in the direct and reverse (shrinkage) deformation processes almost coincide (Figs. 7, 8). Note that it is the assumption of the equilibrium deformation of a polymer that is the basis for the statistical theory of high elasticity [7].

Let us now consider the structural rearrangements of a polymer that is in the rubbery state and contains a system of chemical crosslinks (Fig. 9). The micrographs show that the direct stretching of NR exhibits the same behavior as the deformation of other similar systems [15, 22] (Fig. 2). In the studied range of stretching ratios, deformation leads to the occurrence of a regular microrelief and fragmentation of the coating. An increase in the stretching ratio of the polymer results in a decrease in the period of the microrelief and a decrease in the average size of fragments of the failed coating in full accordance with the previously developed concepts [15–20].

An attempt to form a stable microrelief on the surface of crosslinked rubber revealed some previously unknown general relationships (Fig. 10). As before, we

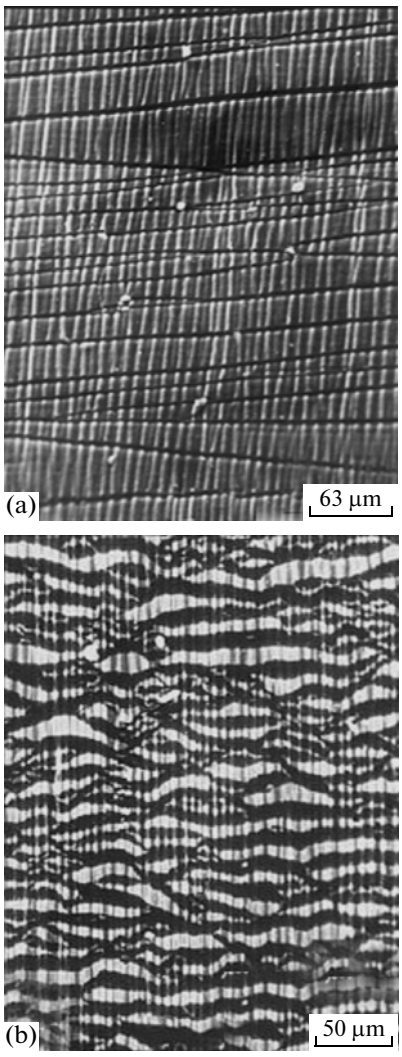

Fig. 9. Scanning electron micrographs of samples of crosslinked isoprene rubber with a platinum coating stretched by (a) 25 and (b) 400%.

deformed the polymer sample to the desired elongation ratio, fixed its dimensions, deposited a metal coating, and released the sample from the clamps of a stretching device. Owing to stress release, the sample completely recovered its dimensions, an result that was accompanied by formation of a microrelief in the deposited coating [21].

It was found that this relief significantly differs from the microreliefs previously observed during deformation of other systems, in particular, PVC (Fig. 8). These unknown features of surface structure formation are the most pronounced at low stretching ratios. Figure 10a shows the micrograph of a rubber sample subjected to 10% stretching with subsequent deposition of a metal coating and release of mechanical stress. The result is that the sample's dimensions completely decrease. It is evident that, in this case, a microrelief consisting of a few structural elements is formed on the polymer surface. The elements are parallel folds that form, as in other cases, a regular microrelief. However, these folds are assembled in fairly well bounded "packages" within which the folds are arranged regularly and parallel to each other.

During the direct stretching of the same polymer with the same coating (Figs. 9, 10), the regular cracking of the coating and the formation of a regular microrelief are significantly different. The analysis of the results presented in Fig. 10 suggests that the deformation mechanism of the crosslinked rubber is greatly different during the direct stretching of the polymer and its shrinkage. According to the statistical theory of high elasticity [7], the deformation of a crosslinked rubber network is affine and at equilibrium and must not differ, regardless of whether the polymer is stretched by an external force or undergoes spontaneous contraction.

The above-discussed experimental data suggest that, during the deformation and shrinkage of a crosslinked rubber, the used technique reveals some previously unknown features. It is important to note that surface structure formation in rubber–metal coating systems is greatly different during the direct stretching of a polymer with a coating and during the shrinkage of the same polymer with a coating deposited in the deformed state (compare Figs. 9 and 10). Thus, this technique makes it possible to determine that, under the conditions of the experiment conducted in [21], the deformation of rubber is not at equilibrium. This circumstance is evidenced by the noncoincidence of the patterns derived in the study of the direct deformation (stretching) and reverse deformation (shrinkage) of the polymer. The revealed differences are probably due to the orientational crystallization of this polymer [23]. At the same time, during the deformation and shrinkage of the plasticized PVC, these strong differences are not observed, a result that is indicative of a greater closeness of the deformation of this polymer to equilibrium.

In-Plane Deformation

Important information about the deformation mechanism of rubbery polymers is provided by the study of their in-plane deformation and shrinkage. The in-plane stretching of polymer films was performed as follows [24]. A polymer film was mounted in a circular frame. The deformation of the film was performed with a punch that was pushed to a required distance in the hole of the circular frame normal to the plane of the film. As a result, the film was stretched in the plane to a desired extent. After stretching, the sample dimensions were fixed with a circular clamp, and a thin (10 nm) layer of platinum was deposited on their surface via ion-plasma spraying. Then, the samples were released from the clamp, and their surface was examined with a scanning electron microscope. In all

cases, after the samples were released from the clamps, they completely recovered their original dimensions.

Figure 11 shows the electron micrographs of the plasticized PVC samples subjected to in-plane stretching to different strains and the subsequent deposition of a thin (10 nm) metal (platinum) layer on their surface and shrinkage. It is clear that, during the in-plane compression (shrinkage) of the PVC film subjected to in-plane stretching, the metal coating deposited on the polymer surface loses its stability and assumes a regular microrelief. The pattern of formation of this relief is fully consistent with the morphology of the reliefs that occur during the in-plane shrinkage of other polymers [25–29]. The figure shows that this microrelief is composed of closely packed randomly curved folds that uniformly cover the entire surface of the polymer. The widths of these folds are fairly homogeneous and can be measured in the presented micrographs.

An increase in the in-plane stretching ratio from 14 to 27% does not introduce fundamental changes into the morphology of the microrelief that occurs during shrinkage (Fig. 11). It is only the value of the fold period that changes. It was shown in [30] that the number of folds does not depend on the compression ratio of the polymer substrate. At the initial moment of the loss of stability of the coating, a certain number of folds originate on the entire surface of the polymer; during further compression of the polymer substrate, their number does not increase. It is only the compression of the resulting relief that occurs by analogy with the compression of accordion bellows.

Thus, during the in-plane shrinkage of the plasticized PVC, owning to a decrease in the surface area of the polymer, the deposited coating, according to the known relationships [15–20], loses its stability and assumes a regular microrelief. It is important that this relief is morphologically uniform. This result is indicative of the affinity of the stress field responsible for the shrinkage of the deformed polymer and, hence, the relative homogeneity of the structure of the polymer substrate.

Let us now consider the results of studies of similarly prepared samples of classical elastomers, i.e., crosslinked rubbers (NR and SIR). Figure 12 shows the scanning electron micrographs of the NR samples prepared via the above-described technique. It is clear that, at relatively low values of in-plane compression, a regular microrelief similar to that observed in the PVC occurs on the polymer surface during shrinkage (compare Figs. 11 and 12a). However, at higher compression ratios (Fig. 12b), new morphological features of the resulting microrelief are revealed. Along with zones of the unordered arrangement of folds, zones in which folds are consistently arranged appear on the polymer surface. These zones have a length of 20–40 μm and are separated by zones with the unordered arrangement of folds with approximately the same size.

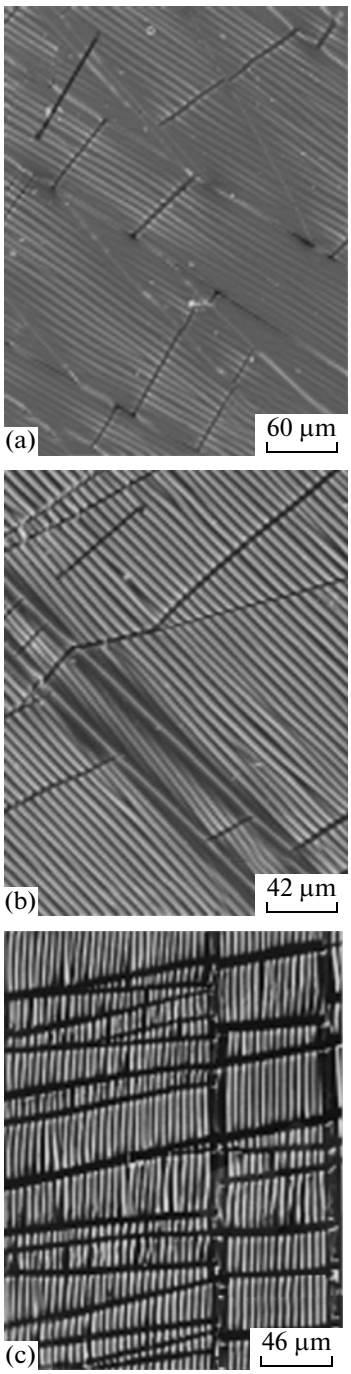

Fig. 10. Scanning electron micrographs of samples of crosslinked isoprene rubber that were stretched by (a) 10, (b) 20, and (c) 100%; that were deposited with a platinum coating; and that were shrunk to the initial state.

Regular relief patterns that occur during the deformation (shrinkage) of polymers with a thin coating deposited on their surface provide a basic visualization of the stress fields responsible for these processes. It may be suggested that, at least for rubbers, that these

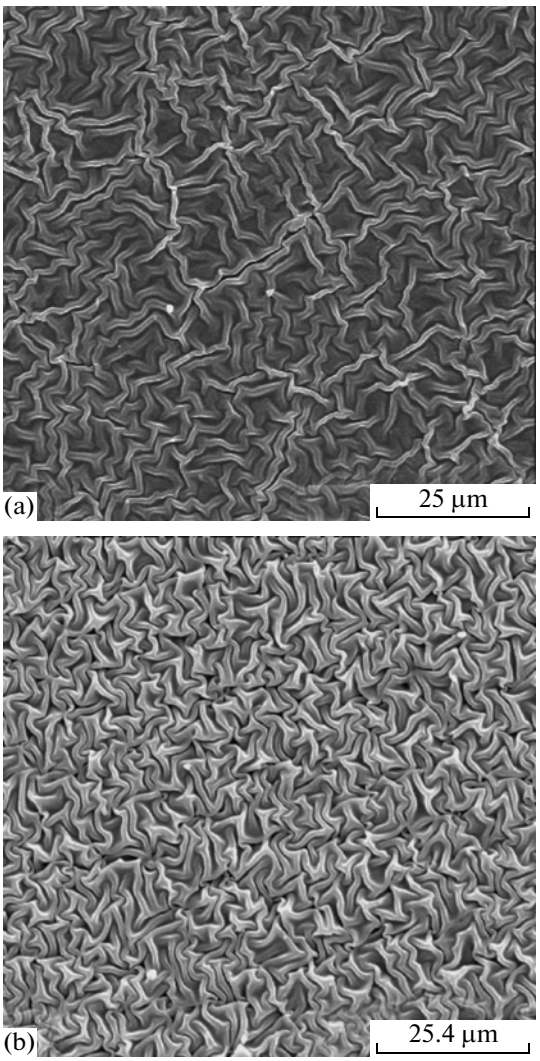

Fig. 11. Scanning electron micrographs of plasticized PVC samples deformed under in-plane stretching by (a) 14 and (b) 27% that recovered their original dimensions after the deposition of a thin (10 nm) layer of platinum on their surface.

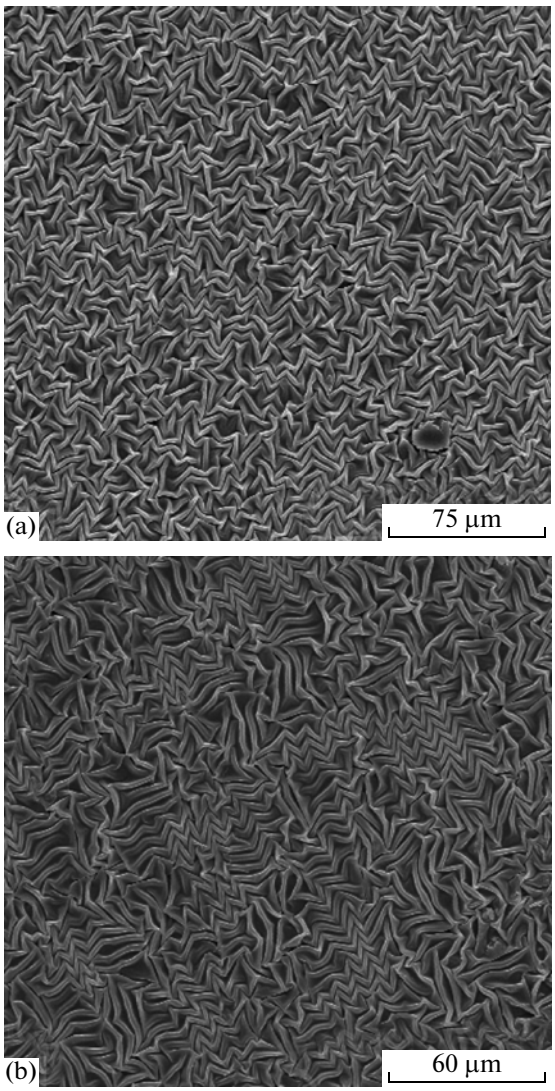

Fig. 12. Scanning electron micrographs of NR samples deformed under in-plane stretching by (a) 5 and (b) 20% that recovered their original dimensions after the deposition of a thin (10 nm) layer of platinum on their surface.

fields are homogeneous (affine), a circumstance that is the basis for the statistical theory of high elasticity [7]. The homogeneity of the microrelief pattern that occurs during the compression of a coating on a pliable base is probably indicative of a uniform stress field responsible for the in-plane shrinkage of the polymer. It is this pattern that is observed during the in-plane shrinkage of plasticized PVC. At the same time, the study of the shrinkage of crosslinked rubbers reveals two types of morphological varieties of regular microreliefs: those with an unordered arrangement of folds and those with a regular arrangement of folds (Fig. 12). This circumstance means that the stress field responsible for the shrinkage of polymers is nonuniform, and, hence, the spatial structure of the rubber is inhomogeneous. Moreover, the used technique makes it possible to visualize and estimate the dimensions of these structural inhomogeneities (20–50 μm). Note that differences in the patterns of surface structure formation between plasticized PVC and crosslinked rubbers were previously found under conditions of uniaxial stretching (shrinkage) of these polymers [21]. (See the previous section.)

This outcome leads to a question about the mechanism of this phenomenon: What is the cause of differences in the microrelief patterns that occur during the shrinkage of plasticized PVC and chemically crosslinked rubbers? Flexible PVCs with a high content of plasticizer are composed of linear nonbranched macromolecules. Commercial samples of PVC exhibit a low degree of crystallinity, which is explained by a low amount of syndiotactic sequences in its chains.

Nevertheless, the presence of small regular sequences of elementary units is responsible for the possibility of local interchain crystallization of the polymer, which is sufficient for formation of a spatial network of macromolecules linked together through crystalline junctions in solutions [31]. This fact makes this polymer similar (reversibility of large deformation) to classical elastomers. An analysis of Fig. 13 indicates that this network has a spatially homogeneous structure.

The experimental electron micrograph shown in Fig. 13 confirms the available literature data that do not make it possible to consider classical elastomers (crosslinked NR and SIR) in the form of topologically homogeneous networks. In particular, the theoretical calculations represented in [32] make it possible to understand the mechanism of inhomogeneous swelling and the resulting inhomogeneous distribution of stress and strain in network polymers. The microheterogeneous structure of SIR was revealed via direct large- and small-angle X-ray diffraction [33]. According to the ideas outlined in [34, 35], one of the causes of the heterogeneity of the network may be the presence of inhomogeneities in the system even before the vulcanization stage. It was shown in [36] that NR contains sol and gel fractions. The gel fraction is composed of macromolecules with $M > 10^6$ and aggregates of linear macromolecules that which arise because of the presence of polar oxygen-containing groups. The amount of this gel is not constant and is dependent on the history of the studied sample [36–38]. At the same time [39, 40], the plasticization of NR, which is performed to improve its properties, likewise leads to the formation of a gel fraction composed of weakly crosslinked rubber particles.

Thus, the plasticization process, which occurs prior to the chemical crosslinking (vulcanization) of rubbers, results in a product with an inhomogeneous composition. The subsequent vulcanization fixes this spatial inhomogeneity via chemical bonds. In order to elucidate the nature of the structural heterogeneity of the studied rubbers, the identification and quantitative estimation of the gel fraction in plasticized NR was studied in [15–17]. It was found that these systems are not solutions of linear macromolecules, because a portion of the polymer is present in the solution in the form of swollen microgels with a size of 2–3 μm. The separation of these microgels from the noncrosslinked fraction of the NR with the use of an ultracentrifuge made it possible to find that their content is 25–30% of the weight of the NR. These data are consistent with the results from [41, 42], which revealed that, during the plasticization of rubbers, the longest macromolecules undergo scission and partial crosslinking. Depending on the plasticization mode, the content of the gel fraction can achieve 60% of the weight of the original NR [43].

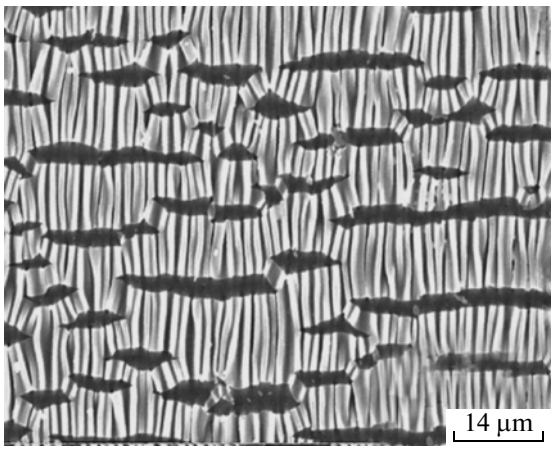

Fig. 13. Scanning electron micrograph of a PVC sample stretched by 100% at 90°C, the surface which, after cooling to room temperature at fixed dimensions, was coated with a thin layer of platinum and then annealed at 100°C.

The used microscopic technique makes it possible to visualize the structural features of the deformation of rubbery polymers and is very sensitive to the structural (spatial) heterogeneity of the deformed elastomer. This technique makes it possible not only to reveal the structural (topological) heterogeneity of a rubber network but also to estimate the size and location of these structural heterogeneities, a step that is extremely difficult or even impossible to do by other means.

VISUALIZATION OF THE STRUCTURAL REARRANGEMENTS THAT OCCUR DURING ANNEALING OF AMORPHOUS POLYMERS ORIENTED ABOVE THE GLASS-TRANSITION TEMPERATURE

It is known that the annealing of polymers oriented above T_g is accompanied by their almost complete shrinkage during annealing. Using the technique for visualizing the structural rearrangements, we analyze the shrinkage of two polymers deformed above their values of T_g. After deformation, the polymers were cooled below their values of T_g and released from the clamps of the stretching device. Next, the sample surface was coated with thin metal layers and annealed above T_g (100°C). The sample surface was examined with an electron microscope. Figure 13 presents the data obtained for PVC that suggest that the shrinkage of the polymer causes multiple fragmentations of coatings and the formation of a regular microrelief. The fragmentation is attributed to the lateral expansion of the samples during shrinkage of the oriented polymer. The regular microrelief is induced by the uniaxial compression deformation of the coating during its shrinkage. The shrinkage of this sample during annealing was almost complete (92%) and indepen-

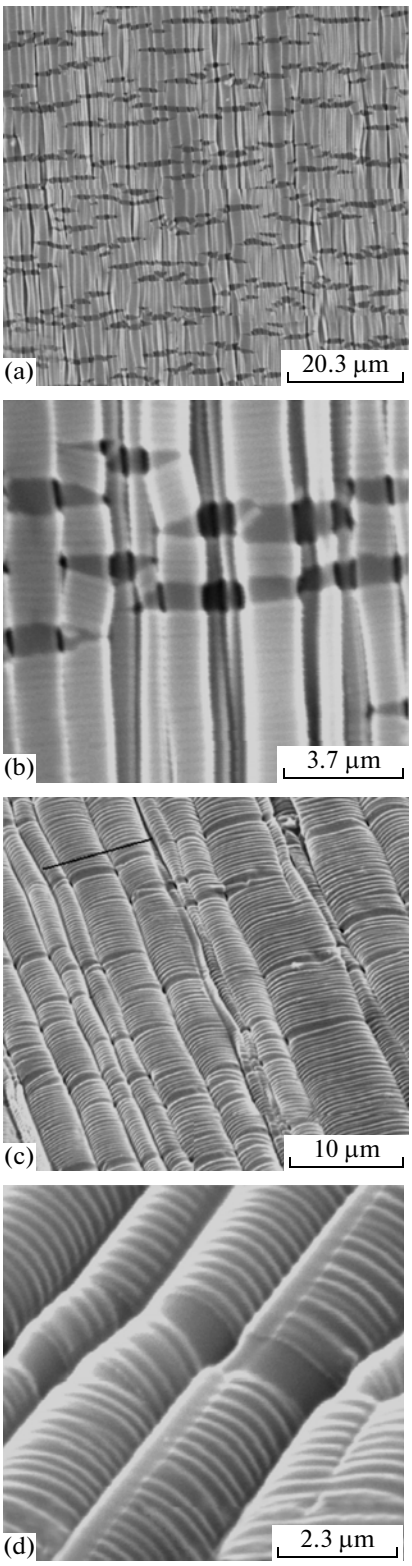

Fig. 14. Scanning electron micrographs of a PET sample stretched by 100% at 90°C, the surface which, after cooling to room temperature with fixed dimensions, was coated with a thin layer of platinum and then annealed at 100°C. The micrographs were taken during (a, b) the perpendicular and (c, d) inclined position of the sample with respect to the axis of the electron beam.

dent of the rate of stretching of the polymer for its orientation above T_g, although this crystallization occurs at a higher rate of stretching [44, 45]. The aforementioned fact is indicative of the high rates of the relaxation processes that accompany the deformation of the polymer above T_g. This circumstance confirms the previous conclusion that the deformation of PVC occurs under conditions close to equilibrium.

The study of the PET samples treated under the same conditions as those of the PVC yielded crucially different results. It is important that the value of shrinkage of the PET samples during their annealing at 100°C was 95%; i.e., it was no different from the shrinkage of the PVC. Despite this coincidence, it was found that the used technique makes it possible to reveal a number of morphological features of the microrelief that occurs during the shrinkage of the PET samples with a coating that are not observed in the study of corresponding PVC samples. The shrinkage of PET is accompanied by structural rearrangements that, at first glance, are qualitatively similar to those discussed above for the case of PVC (Fig. 14a). The formation of a regular microrelief and multiple fragmentations of the coating are observed for all the studied samples. As in the case of PVC (compare Figs. 13 and 14a), many short cracks oriented perpendicularly to the direction of the folds of the microrelief are observed in the coating.

A consecutive magnification of the images of the microrelief of the PET samples that underwent shrinkage during annealing reveals the pattern of their fairly unusual structure formation (Fig. 14b). First, as was noted above, there is a wide variation in the wavelength of the resulting microrelief, due to which it largely loses its regularity relative to the relief derived during the direct stretching of the polymer and the shrinkage of the PVC samples. Second, each fold of this relief is covered with a remarkably regular microrelief that has a significantly lower period (0.27 μm). This regular microrelief covers the entire surface of the irregular folds perpendicular to their major axis. These folds are so regular that they resemble stacks of coins (Fig. 14b).

This amazingly beautiful structure is the most pronounced if the sample is inclined relative to the direction of the electron beam (Fig. 14c). At high magnifications, it is evident (Fig. 14d) that the irregularities that look like cracks in the coating (Figs. 14a, 14b) are fragments of large folds that do not have a regular relief and have a smooth surface. What are the causes of the revealed phenomenon?

To answer this question, we measured the dimensions of the annealed samples. It was found that, although the finite dimensions of the samples of the two polymers derived via annealing were almost identical, the ways in which they achieve these dimensions were substantially different (Fig. 15). While the PVC exhibits the usual thermomechanical behavior charac-

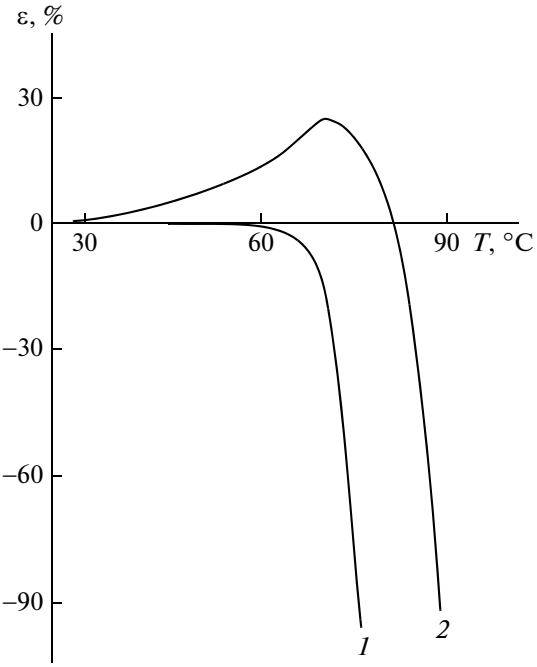

Fig. 15. Annealing-temperature dependence of the relative change in the lengths of (*1*) PVC and (*2*) PET samples deformed above their T_g values (100°C).

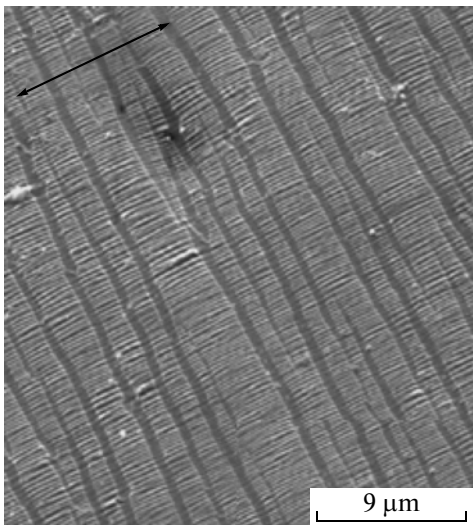

Fig. 16. Scanning electron micrograph of an oriented PET sample that was annealed 65°C and that had a deposited thin (11 nm) metal coating on its surface. The arrow shows the direction of self-elongation of the sample.

teristic of oriented amorphous polymers (shrinkage during annealing), the shrinkage of the PET is preceded by the self-elongation in the direction of the axis of prestretching. To verify this result and to characterize the process of the found self-elongation, we studied the PET samples annealed at 65°C. (The maximum self-elongation is shown in Fig. 15.) The result of this study is presented in Fig. 16.

It is evident that the PET sample in fact undergoes self-elongation during annealing, an outcome that is clearly evidenced by the pattern of surface structure formation. The sample not only elongates in the direction of the tensile axis, as indicated by the fragmentation of the coating, but also undergoes contraction in the normal direction, a result that is indicated by the formation of a regular microrelief. The formation of the structure shown in Fig. 14 becomes clear now. The fact is that the polymer whose structure is shown in Fig. 16 is subjected to shrinkage. Thus, initially, the polymer without the metal coating undergoes shrinkage in the gaps between the coating fragments, thereby subsequently leading to the compression of these fragments with the result that they "swell" and the pattern shown in Fig. 14 appears.

The self-elongation of oriented PET during annealing was repeatedly observed previously. In particular, it was shown [46, 47] that the amorphous PET stretched below T_g via the mechanism of classical crazing in an absorptionally active liquid medium undergoes significant self-elongation during annealing. The change in the geometric dimensions of uniaxially oriented PET samples was studied in [48]. The samples were prepared via coextrusion through an Instron rheometer at 50–105°C to a draw ratio of 4.4. The use of extrusion deformation made it possible to smoothly vary the strain ratio of the polymer below its T_g. Self-elongation during annealing is observed only for the polymer deformed by 100%, whereas only its shrinkage occurs for other strain values. A few more studies are concern with this phenomenon [49–52].

It is important that, in the above case, the finite dimensions of the annealed samples of PVC and PET were almost identical and self-elongation was found only owing to the used technique of visualization of structural rearrangements of a polymer during its annealing [53, 54].

VISUALIZATION OF STRUCTURAL REARRANGEMENTS THAT ACCOMPANY DEFORMATION AND HEAT-INDUCED SHRINKAGE OF GLASSY POLYMERS

The use of the technique of visualization of structural rearrangements developed in [11–14] makes it possible to obtain important information on the seemingly thoroughly studied rubbery deformation of polymers. The deformation of glassy polymers is currently understood to a much lesser extent; in connection with this, there is no general quantitative theory of this process. It is no wonder that many features of the deformation mechanism of polymer glasses are still debatable. Below, we discuss in greater detail the results of studying the deformation of glassy polymers via the technique of visualization developed in [11–14].

Rolling

Volume homogeneity is one of the major differences in the deformation of polymers in the rubbery state and the glassy state. At the same time, the deformation of glassy polymers is always inhomogeneous [30, 52–54]. This circumstance is macroscopically shown in the formation and propagation of a neck and/or crazes during the uniaxial stretching of polymers and in the development of shear bands during uniaxial compression [55]. The deformation mechanism of amorphous glassy polymers under rolling conditions has been studied to a much lesser extent [56, 57].

In the few studies of the structural and mechanical behavior of glassy polymers subjected to rolling, it was found that, as in other types of mechanical attack, the deformed polymer completely recovers its dimensions during annealing above T_g. This phenomenon made it possible to use the above developed approach for visualizing structural rearrangements of the polymer deformed under these conditions. In [58], the study was conducted with the use of a glassy PC. PC samples were subjected to rolling at room temperature. After that, their surfaces were coated with thin metal layers and annealed at different temperatures.

The used technique of visualization of structural rearrangements made it possible to reveal that structural rearrangements in the annealed PC begin long before the polymer achieves T_g. (The glass-transition temperature of PC is 145°C.) Figure 17 shows the micrographs of the PC sample subjected to rolling at room temperature and annealed at 110°C after the deposition of a metal coating on its surface. It is clear that, even at this low temperature, a kind of large-scale molecular motion occurs in the polymer, thereby leading to formation of a large number of shear bands that exhibit rectilinear propagation over the polymer surface at an angle to the axis of rolling (Fig. 17a). In addition to the shear bands, a regular wavy relief is clearly seen in the deposited coating, a phenomenon that is indicative of the shrinkage of the polymer in the direction of the axis of rolling.

An increase in the annealing temperature to 120°C leads to further improvement of the folded relief oriented perpendicularly to the axis of rolling (Fig. 17b). The folds of this relief become fairly long and perfect, although they have some "tortuosity." Moreover, a detailed microscopic examination makes it possible to reveal new elements in the surface microrelief. At an annealing temperature of 120°C, a few folds oriented perpendicularly to the axis of the "primary" folds, that is, along the axis of rolling, are formed on the surface of PC.

An increase in the annealing temperature to 140°C is accompanied by "disintegration" of the general pattern of relief formation into well-isolated zones with differently located asymmetric structures (Fig. 17c). High folds oriented mostly perpendicularly to the direction of rolling are clearly seen (extended bright bands in Fig. 17c). These folds are surrounded by dark areas, the structure of which will be discussed below. The rest of the polymer surface is covered with the folded structure on a smaller scale.

Finally, the annealing of PC that has a deposited coating and that was subjected to room-temperature rolling at a temperature above its T_g (155°C) leads to the occurrence of a uniform microrelief in its surface with two mutually perpendicular structures that covers the entire surface area of the polymer (Fig. 17d). We emphasize that, at this annealing temperature, the polymer completely recovers its original dimensions.

The above-presented variety of morphological forms occurs in PC during its annealing below T_g, that is, "within" the glassy state of the polymer, a circumstance that is indicative of the occurrence of some kinds of large-scale molecular motion in this temperature range. The relaxation of these types of molecular motion during annealing leads to a complex evolution of the internal stress that is clearly detected via the used technique of sample preparation for microscopic studies.

This technique makes it possible to reveal two structural modes of the heat-induced relaxation of PC subjected to rolling. As the annealing temperature increases (~100°C), the strain relaxation begins and folds directed normal to the axis of rolling are formed in the coating. Once the annealing temperature achieves 130°C, the second deformation component appears. The direction of this component is normal to the direction of the first component and the direction of rolling, and this portion of deformation is detected in the form of folds oriented along the axis of rolling. Further annealing is accompanied by the relaxation of the two components, as evidenced by the occurrence of two mutually perpendicular morphological forms of microreliefs in the coating. These data do not provide an answer to the question why only two mutually perpendicular components of inelastic deformation, one of which coincides with the direction of rolling, occur during rolling. This result is not obvious, because, during rolling, the polymer film is free along its entire perimeter and there are no obstacles to its orientation in any direction.

Uniaxial Stretching and Compression of Glassy Polymers

The deformation of glassy polymers exhibits some features that do not fit any conventional concepts of glassy polymers in which large-scale molecular motion is frozen [1–6]. These features include the phenomenon of stress relaxation in the polymer in the elastic so-called Hookean region of the stress–strain curve [1], the increase in stress in a deformed glassy polymer during its isometric annealing in the temper-

ature range below T_g [59, 60], the low-temperature (below T_g) shrinkage of a deformed polymer glass in the strain range below its yield point [61], the storage of internal energy in a deformed glassy polymer in the strain range below the yield point [62], some anomalies of thermophysical properties [63–65], and other phenomena.

It is no wonder that today there are several alternative views on the mechanism of inelastic deformation and heat-induced recovery of polymer glasses. A series of studies of the heat-induced recovery of deformed polymer glasses can be regarded as the first approach [61, 66–68]. In these studies, anomalies of the mechanical behavior of polymer glasses are attributed to their original structural heterogeneity. It is assumed that the mechanism of high-temperature recovery is associated with the entropic relaxation of excited stretched macromolecular coils and their transition into their original state that are due to the thawing of the segmental mobility at T_g of the polymer. In other words, the recovery of the oriented polymer is observed at T_g. The nature of the low-temperature component of recovery was attributed to conformational rearrangements of macromolecules induced by the joint action of temperature and internal stress stored during deformation.

The second approach to explaining the same structural and mechanical characteristics of polymeric glass is presented in [62, 69, 70]. The model is based on a concept according to which the total inelastic deformation and steady-state plastic flow occur in a polymer structure saturated with small-scale plastic shear transformations (PSTs) rather than in the original structure. The former structure is excited and metastable. The formation of PSTs begins at the earliest stages of loading and reaches a steady state at low strains (20–35%). PSTs are nonconformational nonvolume shear entities surrounded by elastic stress fields; they are the main source of macroscopic deformation. Conformational rearrangements in the chains at $T < T_g$ do not occur directly under the action of stress; they are the products of death of PSTs. It is assumed that the total energy stored in the sample during deformation is concentrated in these fields. The relaxation, physical aging, and molecular motion in the deformed glass are closely related to the birth and death of PSTs. The mass transfer during the deformation of glass is provided by small-scale motions of the γ, β, and possibly δ types, rather than by segmental motions.

In some studies [63, 71, 72], the plasticity of polymers below their values of T_g is associated with the β molecular motion. In addition, we can mention studies [73–75], in which the plastic deformation of a solid polymer is described via the concept of free volume. In the above-cited studies, the mechanism of plastic deformation is considered at a microscopic submolecular level. It is assumed that, in all cases, plastic defor-

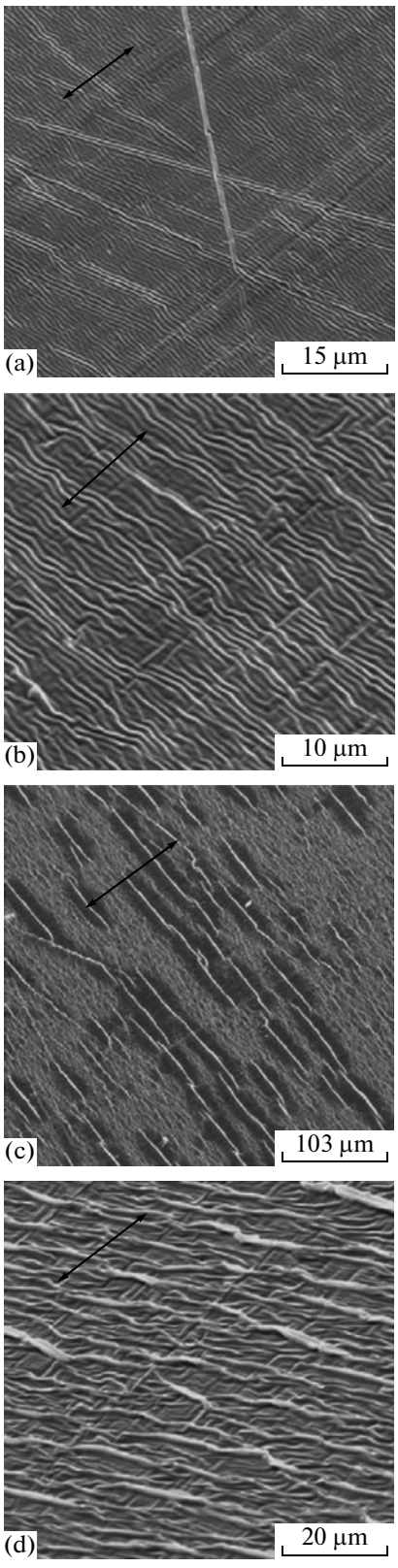

Fig. 17. Scanning electron micrographs of PC samples subjected to rolling at room temperature with the subsequent deposition of a thin (10 nm) platinum coating on their surface. The samples were annealed at (a) 110, (b) 120, (c) 140, and (d) 155°C. The direction of rolling is shown by an arrow.

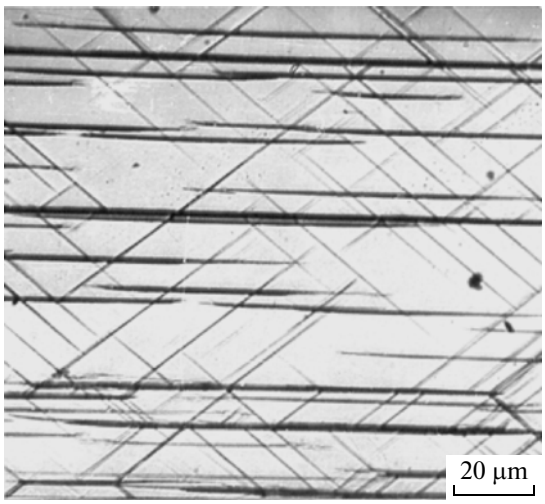

Fig. 18. Light micrograph of a PET sample deformed at room temperature under a constant load of ~0.7 of the yield point for 2 h [30].

mation is delocalized over the volume of the polymer and that its elementary act occurs in volumes of tens to hundreds of angstroms. It is possible that the availability of several alternative explanations for the same phenomenon is due to the fact that these viewpoints are not based on direct structural data.

In fact, the plastic deformation of glassy polymers is fundamentally inhomogeneous and evolves, at least at early stages, in local zones. This effect can be easily shown with an optical microscope. The inhomogeneities of the plastic deformation of a glassy polymer, for example, are easily detected in the range of strains that do not exceed the yield point. It was found in [76] that, for a draw ratio of 3–5% for PC and PVA, at temperatures 10–20°C lower than the respective glass-transition temperature, intense diffuse X-ray scattering occurs. This result clearly indicates that, under these conditions, a discontinuity of the glassy polymer and the formation of interfaces, which are sources of small-angle X-ray scattering, occur in the Hookean region of the stress–strain curve. Lazurkin was the first to note that the deformation of the polymer becomes volume-inhomogeneous in the yield region [1]. A system of inhomogeneities that are easily detected with an optical microscope and even with the naked eye is formed in the polymer. These inhomogeneities are straight lines that intersect the polymer at an angle of 45°–55° with respect to the tensile axis. By analogy with low-molecular-mass solids, Lazurkin called them shear bands and noted that their occurrence requires the presence of microscopic inhomogeneities (stress concentrators).

These shear bands are easily detected via direct microscopic examination. Figure 18 presents the light micrograph of a sample of glassy PET aged under a constant tensile load of 0.6 of the yield point. The figure shows that, along with a system of shear bands oriented at an angle of ~45° with respect to the tensile stress, other zones of the plastically oriented polymer that propagate perpendicularly to the axis of tensile stress are observed in the polymer. These are so-called crazes. They differ from shear bands not only by the direction of propagation but also by the presence of microvoids in their structure [10].

In addition, the zones of the plastically deformed polymer develop under conditions of its stretching at a constant rate. Figure 19 presents the light micrograph of a PET sample deformed at room temperature until neck formation. The portion of the sample that has not yet transitioned into an oriented state (neck) is riddled with shear bands. The material of the neck does not contain these bands at first glance. It is evident that the shear bands that occur in the undeformed portion of the polymer adjacent to the neck disappear (dissolve in it). Nevertheless, this material "remembers" that the transition into a neck is undertaken by the polymer that contains shear bands. If a neck of PET is exposed to a solvent in which the polymer swells, the shrinkage caused by this treatment will lead to the formation of a system of shears in the material [77].

The above-described microscopic technique makes it possible to trace the "fate" of these bands after their absorption by the neck. For this purpose, we studied PET samples with a thin (10 nm) platinum coating. Figure 20a depicts the micrograph of the region of the polymer localized at the interface between its neck and the nonoriented portion. In this location, the sample thickness sharply decreases, thus leading to a fairly sharp bend of its surface that was initially plane. This bend is naturally accompanied by the cracking of the coating. At the same time, this technique allows visualization of the formation of shear bands in this region. It is clearly that these bands undergo rectilinear propagation through the specified transitional zone at an angle of ~45° to the axis of tensile stress.

The transition layer between the nonoriented portion of the polymer and the propagating neck, in proportion to its deformation, moves along the sample until its complete transformation into a neck. Figure 20b depicts the portion of the sample with a fragment of the transition layer and the portion of the sample that has transformed into a neck. This technique makes it possible to visualize the structural evolution of shear bands during their absorption by the neck. It is clear that the shear bands formed in the transition layer reach the region of the neck and, after the incorporation into the "material" of the neck, lose their orientation of 45°C in the direction toward the tensile axis. They unfold almost parallel to the tensile axis and are incorporated into the structure of the neck in this form. These shear bands are clearly seen in the regions at any distance from the zone of transition of the polymer into a neck (Fig. 20c). It is clear that, after

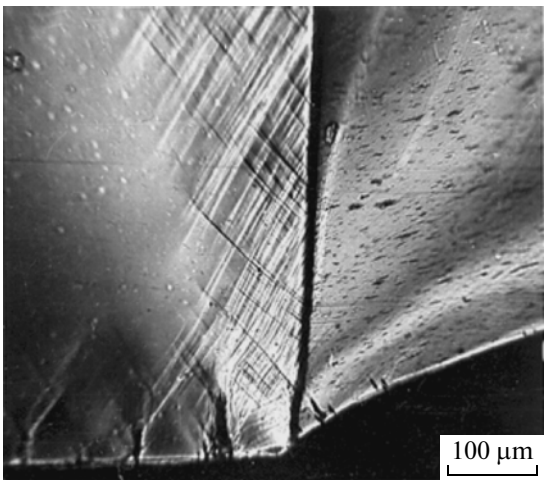

Fig. 19. Light micrograph of a PET sample deformed at room temperature with the formation of a neck. The right-hand side depicts the portion of the sample that has transformed into a neck; the left-hand side shows the undeformed portion of the sample. The photo was taken in crossed polaroids [30].

the incorporation of shear bands into the structure of the neck, we cannot call them shear bands. However, these entities have some structural differences from the rest of the material of the neck. Therefore, the resulting neck during the stretching of a glassy polymer is structurally inhomogeneous.

The deformation of the polymer, which makes it possible to prepare samples for direct microscopic examination, is performed under conditions where the polymer can freely slide with respect to the compressing surfaces. In this case, the height of the sample decreases because of the increase in its surface area that is in contact with the compressing surfaces. It is these surfaces of the sample that change their surface area during the deformation or shrinkage of the sample (Fig. 21). If a thin coating is deposited on the surface of a deformed sample before its annealing (shrinkage), then, subsequently, this coating is representative of the structural rearrangements that occur in the substrate. The preparation of a sample for this study is schematically shown in Fig. 22.

Consider the process of heat-induced shrinkage of two PET samples (T_g ~ 75°C): One of them was deformed under uniaxial compression above T_g of the polymer (100°C); the other, below T_g of the polymer (at room temperature). Note that, although the two prepared samples were annealed to the same temperature (105°C), their pathways to return to their original dimensions were greatly different. Figure 23 shows that the sample deformed at 100°C recovers its dimensionss in the T_g range of PET. At the same time, PET deformed at room temperature recovers its dimensions almost completely in the temperature range below T_g. Another amorphous polymer, PS, exhibits a similar

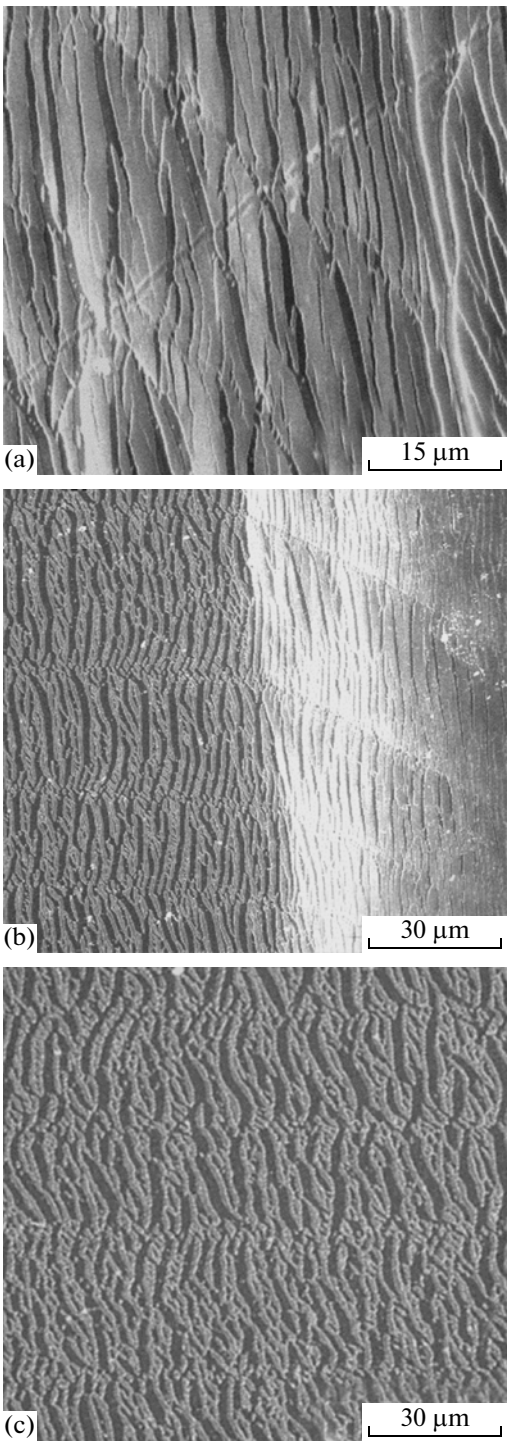

Fig. 20. Scanning electron micrographs of a PET sample with a thin (10 nm) platinum coating stretched at room temperature with the formation of a neck: (a) the region of transition of the polymer into the neck, (b) the portion of the sample in which the transition layer (right) and the region of the formed neck (left) coexist, and (c) the region of the formed neck remote from the transition layer. The tensile axis is horizontal.

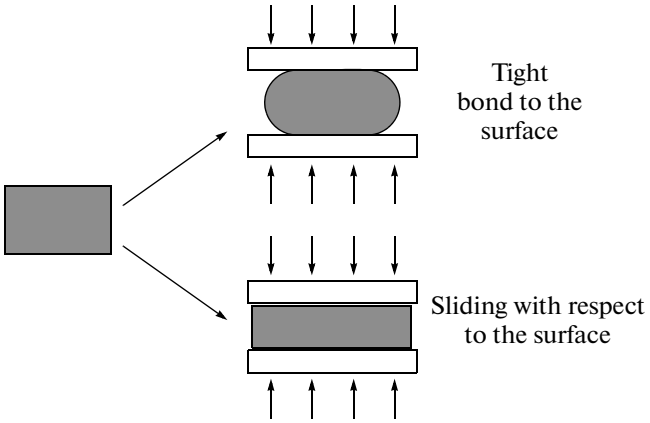

Fig. 21. Schematic representation of the uniaxial compression of a polymer under conditions at which its surface has a tight bond to the compressing surface or freely slides during compression.

behavior [13]. The above thermomechanical behavior of the polymer is fully consistent with the results of studies presented in [61, 62, 67–70].

Figure 24 represents the results of studying two PET samples subjected to in-plane deformation to approximately the same value (22–24%). As was noted above, the only difference between the samples lies in the fact that one of them (Fig. 24a) was deformed above T_g (100°C), while the other was deformed at room temperature (Fig. 24b). Note that, after shrinkage during annealing in the absence of a coating, the surface of deformed samples remains smooth at all stages, regardless of the temperature of predeformation.

The deposition of a coating before the annealing of deformed PET samples makes it possible to reveal and characterize the structural rearrangements of the polymer during its thermal shrinkage [12]. The shrinkage of the polymer in the case of the sample deformed above T_g provides the platinum coating with a regular and pronounced microrelief (Fig. 24a). The mechanism of the occurrence and development of this relief is completely analogous to the above mechanism for other polymers (Fig. 11). This microrelief is uniformly distributed over the entire surface of the sample, a result that is indicative of the general affinity of the in-plane deformation and, accordingly, shrinkage of PET during annealing. It is obvious that the decrease in the interfacial area of the polymer in this case occurs uniformly over its entire surface via bulk diffusion.

Consider now how the deposited metal coating responds to the in-plane shrinkage of PET deformed below T_g. In this case, the heat-induced shrinkage of the polymer is accompanied by greatly different structural rearrangements in the surface layer. It is clear (Fig. 24b) that, owing to heat-induced shrinkage, the entire sample surface is covered with straight stripes that cut across the entire surface of the sample and each other at different angles. Their transverse sizes are not identical; therefore, the width distribution of the stripes is fairly broad. The AFM data (Fig. 25a) show that the stripes are grooves of different widths. Since the observed stripes cut across the entire studied surface of the samples, we can assume that they cut across the entire cross section of the deformed polymer: The wider the stripes are, the deeper they penetrate into the surface of the polymer and vice versa. These stripes are straight channels (Fig. 25b) in which the polymer is drawn from the surface into the bulk.

The experimental conditions are such that, in either case (above and below T_g), owing to the in-plane stretching, the surface of the polymer increases in size (Fig. 22). The increase in the surface area is inevitably accompanied by the "removal" of the material from the depth (bulk) of the polymer to the surface. In the reverse process (shrinkage), the interfacial area decreases; therefore, the polymer is transported from the surface into the bulk. During the deformation of the polymer above its T_g, the deformation of the polymer and the recovery of the previous original surface during annealing uniformly occur with the result that the deposited coating also undergoes uniform compression over the entire surface area. This phenomenon is precisely why a regular relief is formed (Fig. 24a) according to the mechanism discussed in detail in [15–20].

During the in-plane deformation of a glassy polymer, the increase in the surface area is nonuniform. This increase is localized in discrete zones of inelastic deformation, that is, shear bands. The above process occurs via the germination and subsequent broadening of shear bands, precisely as it apparently occurs during

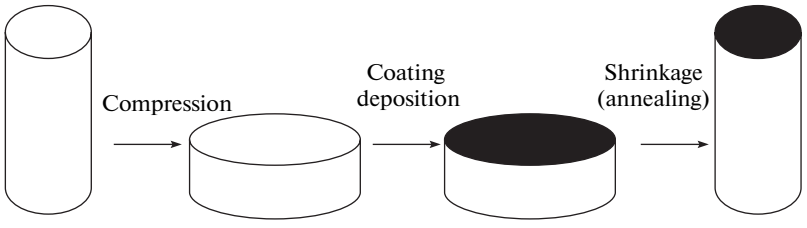

Fig. 22. Experimental design for the visualization of structural rearrangements during the heat-induced shrinkage of a polymer deformed under uniaxial stretching.

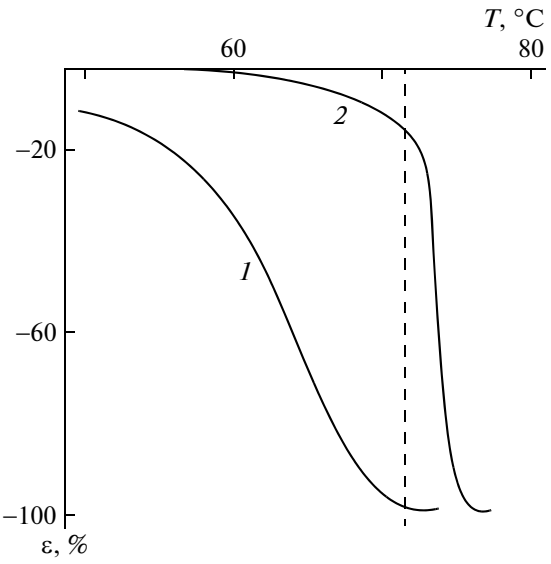

Fig. 23. Recovery of original dimensions during the annealing of PET samples deformed under uniaxial compression at (*1*) room temperature and (*2*) 100°C. The dashed line denotes T_g of PET.

the formation and propagation of crazes [17]. The specified similarity is indicated by the results of microscopic observations, according to which, during the propagation of both shear bands [78] and crazes [17], the deformation process is accompanied by an increase in the number of zones of localized inelastic deformation of the polymer. Thus, in either case, early stages of deformation are characterized by the formation of a polymer material in the form of unoriented blocks of the original polymer that are separated by narrow zones containing a highly oriented polymer and that are isolated from these blocks by well-shaped interfaces.

In addition, the reverse process of thermal shrinkage of the polymer deformed below T_g is nonuniform because the oriented polymer localized in shear bands is responsible for the reversibility of deformation. The results derived via a new microscopic technique ([11–14] and Fig. 24b) show that the shrinkage of the polymer occurs primarily in shear bands, as evidenced by the retraction of the coating into the bulk of the polymer in shear bands (the straight lines in Fig. 25). In other words, the transfer of the material from the surface into the bulk during shrinkage proceeds via its diffusion in the shear bands, which the deformed polymer perfectly "remembers."

Further development of this technique made it possible to obtain important data on the structural rearrangements of a polymer at different stages of its deformation and to characterize the structural rearrangements that accompany the shrinkage of the polymer deformed to different values.

Figure 26 depicts typical results of this study that are representative of the structural rearrangements of PET samples subjected to uniaxial compression deformation by 30%. After the deformation, their surface was coated with a thin (10 nm) metal coating and annealed at different temperatures. It was found that, at an annealing temperature below T_g (up to 70°C), there is significant shrinkage of the polymer; it occurs mostly in shear bands, while the space between these bands remains smooth and undeformed. As the temperature approached T_g, the material localized between the shear bands was involved in deformation. During annealing above T_g, the entire surface of the polymer is covered with folds, a circumstance that is characteristic of the shrinkage of the polymer

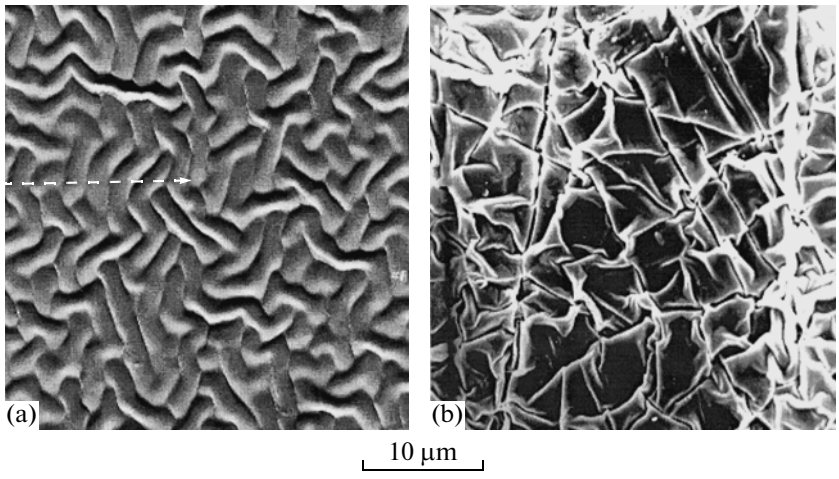

Fig. 24. Electron micrographs of PET samples deformed under uniaxial stretching at (a) 100°C and (b) room temperature. After deformation, thin (10 nm) layers of platinum were deposited on the surface of the samples, and they were subjected to annealing at 105°C [30].

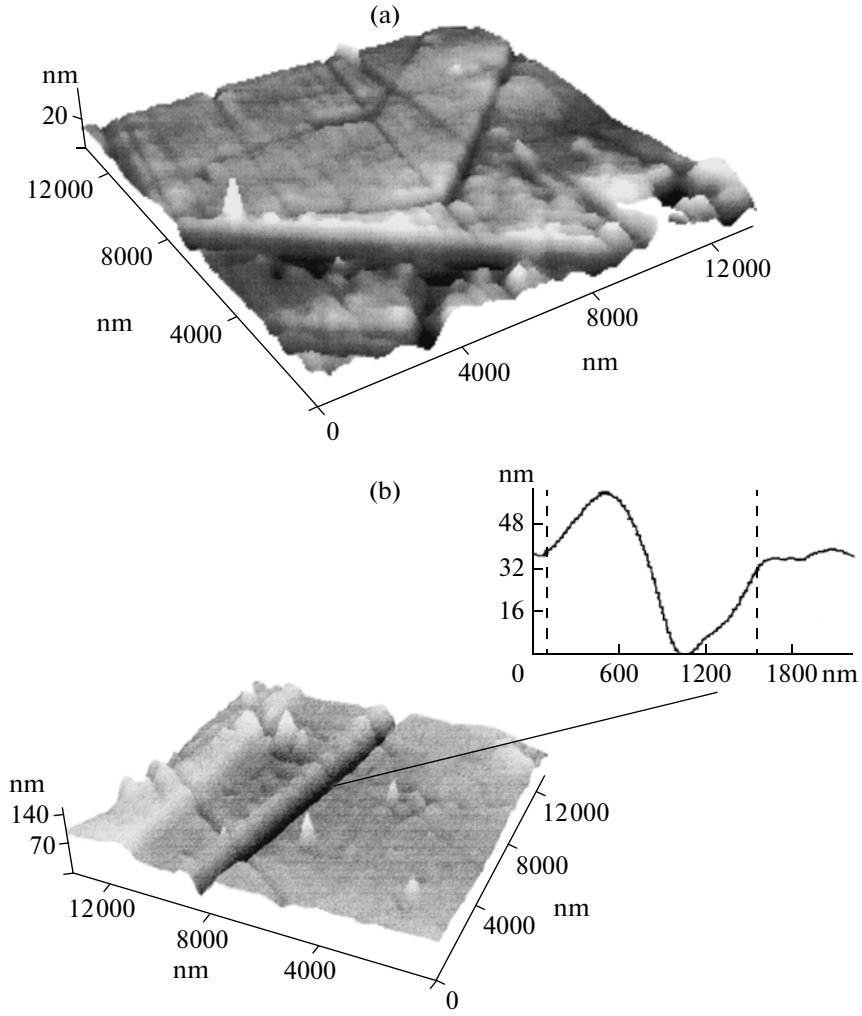

Fig. 25. (a) Three-dimensional reconstruction of the AFM image and (b) the respective profilogram of the surface of a PET sample deformed under in-plane stretching. After the deposition of a thin (10 nm) platinum layer on the surface of the sample, it underwent in-plane shrinkage by 18% during annealing.

deformed above T_g (compare Figs. 24a and 26c). Nevertheless, the shear bands formed at a low shrinkage value (and a low annealing temperature) are identified against the background of the developed folded relief (Fig. 26c).

Similar conclusions were made in the study of the heat-induced shrinkage of PS samples deformed at room temperature. In this case, the experiment was performed somewhat differently. The samples were deformed to the same compression ratio (25%), and a different value of shrinkage was achieved through variation of the annealing temperature. Figure 27 shows the micrographs of PS samples with a platinum coating annealed below T_g at 70°C and above T_g at 90°C. It is evident that the low-temperature annealing results in shrinkage exclusively in shear bands, whereas the annealing above T_g is produced via retraction the material into the bulk over its entire surface. Nevertheless, as in the case of PET, shear bands do not disappear at a high annealing temperature and their network is easily identified against the background of randomly arranged folds.

The above structural data suggest that the recovery of the sample dimensions occurs in different temperature ranges. The samples deformed in the range of low strains (below the yield point and in the yield region) and at a low temperature (below T_g) recover their dimensions during annealing below T_g. At the same time, the polymer deformed to large elongations and in the temperature range above T_g recovers its dimensions in the region of its T_g.

Despite the above-mentioned common features in the mechanisms of inelastic deformation of different glassy polymers, there are certain differences in the methods of sample preparation for the visualization of structural rearrangements of the deformed polymer and the numerous previous studies [61, 62, 67–70]. Usually, the deformation of polymers under uniaxial

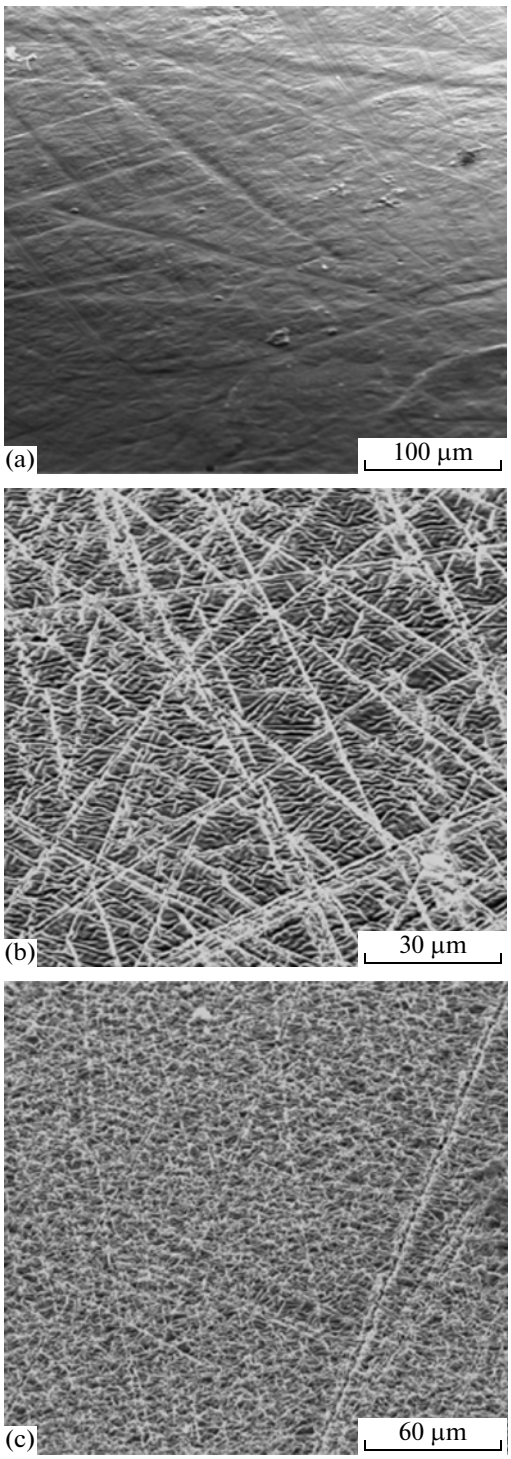

Fig. 26. Scanning electron micrographs of PET samples that were subjected to uniaxial compression deformation by ~30% at room temperature and underwent shrinkage by (a) 2.7, (b) 11.5, and (c) 29.2% during annealing at 50, 60, and 80°C, respectively.

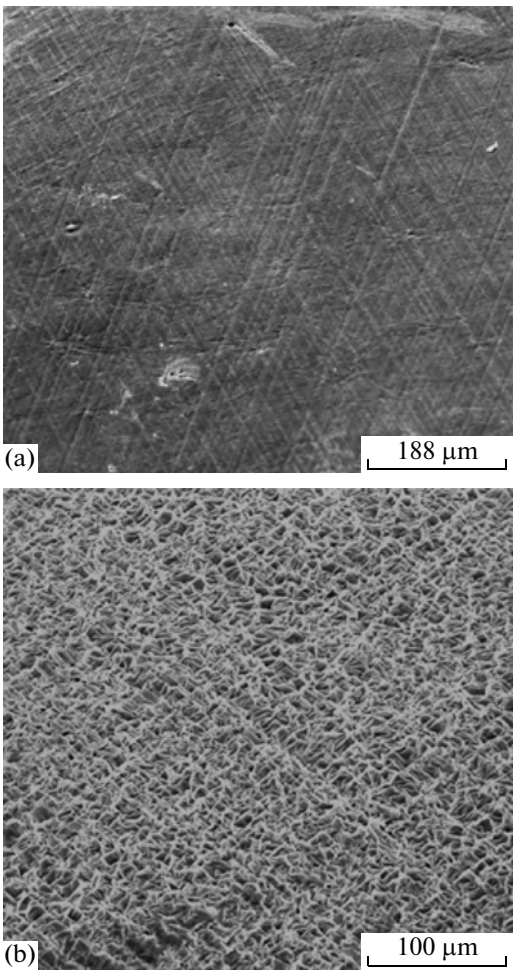

Fig. 27. Scanning electron micrographs of PS samples that were subjected to uniaxial compression deformation by ~25% at room temperature and underwent shrinkage by (a) 7.5 and (b) 25% during annealing at 70 and 90°C, respectively.

compression is conducted with the use of cylindrical samples. After this deformation, the polymer assumes a barrel-like shape. The reverse process of heat-induced recovery of dimensions is studied via measurement of the height of the deformed samples during annealing.

The above-discussed structural rearrangements that accompany the shrinkage of deformed glassy polymers were derived under slightly different conditions [11–14]. In this respect, it is necessary to bring into compliance the data obtained in different ways. Barrel-like samples prepared via uniaxial compression are fairly large, which makes it difficult to use direct microscopic methods. In [55], the technique of thin microsections was used to analyze the morphology of bulk PS samples subjected to uniaxial compression (Fig. 28). It is clear that the PS deformed under uniaxial compression contains zones of the plastically oriented polymer. Since these zones are rectilinear and propagate at an angle of ~45° to the direction of compression, the author of [55] called them shear bands.

These zones contain an oriented polymer because they exhibit strong birefringence in crossed polaroids.

In [14], a new very simple and vivid technique for studying the structural rearrangements of polymers deformed under uniaxial compression was developed. For this purpose, a complete analog of the sample that is usually used for studying the mechanical behavior of polymers under uniaxial compression was prepared. As in [61, 62, 67–70], the sample for tests was a cylinder.

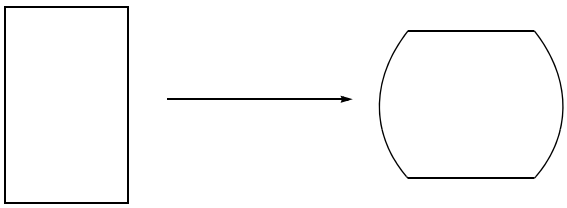

Conventional scheme of deformation of a polymer under uniaxial compression

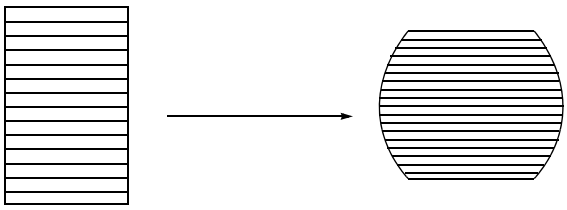

Experimental scheme used to visualize l rearrangements in the polymerstructural rearrangements in the sample under uniaxial compression

However, unlike the commonly used samples, this cylinder was assembled from disks with a thickness of ~1 mm. After deformation, this sample can be disassembled into individual elements, each of which, in turn, can be subjected to analysis via the above microscopic technique. In fact, this is a method of structural tomography of a deformed bulk polymer sample.

It was shown in [14] that the tomographic procedure does not introduce any major changes in the deformation mechanism of the polymer. First, under the action of uniaxial compression, a multilayer sample, the structure of which is shown in the scheme, is deformed as a whole entity, thereby resulting in a change in its shape from cylindrical to barrel-like in full accordance with the change in shape that occurred in [61, 62, 67–70] during the deformation of a monolithic sample. Second, the curve of uniaxial compression of a multilayer sample fully corresponds to the curve of uniaxial compression of a monolithic polymer.

The developed approach makes it possible to obtain new important information about the deformed polymer that makes it possible to study the structural and mechanical behavior of the polymer inside bulk barrel-like samples. Figure 29 shows the compression strain of each layer of the polymer as a function of their location (distance) with respect to the compressing surface. It follows that a polymer deformed under uniaxial compression is fairly inhomogeneous in structure. In fact, a sample of PMMA deformed under uniaxial compression by 30% contains regions that sunbstantially differ from each other in strain. The first three or four layers adjacent to the compressing surfaces contain hardly any residual strain. At the same time, in the central part, which was formed because of the compression of the "barrel," the strain of the polymer exceeds 70%.

The proposed technique makes it possible to study the heat-induced recovery of the dimensions of each of the layers that comprise the specified barrel. These data are shown in Fig. 30 in the form of the annealing temperature dependence of the absolute variation in the height of each of the layers that constitute the barrel. Depending on the location of each layer in the total structure of the sample, three types of thermomechanical behavior are observed. The layers (curves *1*–*3*) with respect to their position from the compressing surface undergo slight changes in size during annealing. Their thermomechanical behavior hardly differs from the original undeformed PMMA; therefore, they were not shown in the figure. The sample (curve *4*) exhibits a pronounced low-temperature component of the heat-induced recovery of dimensions. This component appears at an annealing temperature of ~50°C. It is at this temperature that the recovery of the dimensions of all other fragments of the multilayer sample begins. Moreover, in the samples (curves *5*–*9*), the

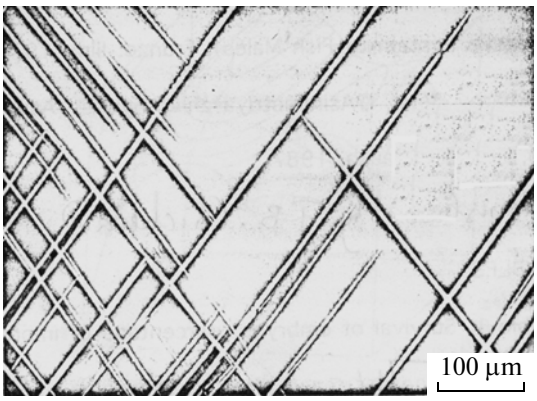

Fig. 28. Light micrograph of a thin section of a PS sample subjected to uniaxial compression. The compression axis is vertical [55].

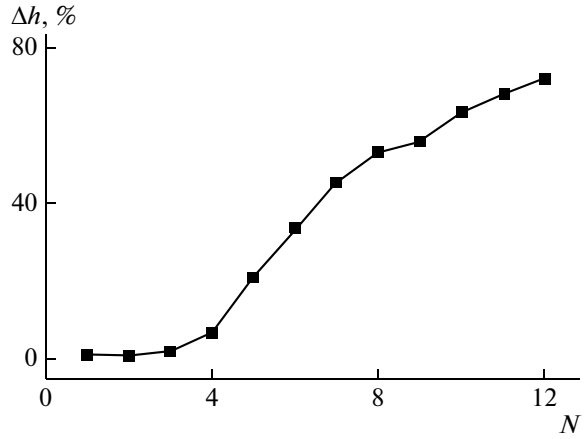

Fig. 29. Uniaxial compression strain of individual PMMA layers (the initial thickness of each layer is 1 mm) versus their position with respect to the compressing surface. The total uniaxial compression strain of the multilayer sample is 30%.

high-temperature (in the region of T_g of PMMA) component of the heat-induced recovery of dimensions appears and becomes increasingly substantial. As the distance from the surface of the barrel increases, this contribution to the heat-induced shrinkage continuously increases and gradually begins to exceed the low-temperature component in absolute value.

The deformation of the cylindrical polymer sample that is usually used in experiments on the uniaxial compression of polymers is fairly inhomogeneous. Inside the sample subjected to uniaxial compression, there are zones deformed to different degrees. These layers in Figs. 29 and 30 not only differ in strain but also differently respond to the subsequent heating in experiments on annealing. The data make it possible to greatly refine the research results derived during the heat-induced recovery of bulk samples. Since a polymer that underwent deformation under uniaxial compression and has a barrel-like shape contains regions that differ in the compression ratio, it cannot uniformly respond to the actual load and, therefore, cannot uniformly recover its dimensions during annealing.

Figure 31 shows the experimental data derived via the heat-induced recovery of dimensions of the PMMA samples deformed at room temperature under uniaxial compression [66]. In this figure, the low-temperature contribution (below T_g) and the high-temperature contribution (in the region of T_g) are compared with the curve of uniaxial compression of PMMA. It is evident from the figure that the low-temperature contribution appears and increases only up to the strain that corresponds to the yield point of the polymer. Further deformation initiates the occurrence of and an increase in the high-temperature contribution (in the region of T_g) to the heat-induced recovery of the polymer. If we compare Figs. 30 and 31, we can see that the low-temperature contribution to the heat-induced recovery of the deformed polymer is made primarily by the layers of the barrel-like polymer which were least deformed (below the yield point and in the yield region of the polymer).

The advantages of the tomographic approach are not limited to obtainment of new information on the mechanical and thermomechanical response of the studied systems. A combination of the tomographic approach with the previously developed technique of the visualization of structural rearrangements [11–14] makes it possible to "peep into" the bulk of the deformed polymer. In fact, after a multilayer sample undergoes deformation, it can be "disassembled" into its constituent elements. The surface of each element can be decorated via deposition of a hard coating and studied through a direct microscopic method after annealing and resulting shrinkage.

These experiments have been performed and their results are presented in Fig. 32. It is clear that the layer (curve *3*) located relatively close to the compressing surface is slightly deformed; therefore, its shrinkage is low (1.7%). The shrinkage of this sample occurs via the retraction of the polymer located on its surface into the bulk in pronounced shear bands. An increase in strain and shrinkage up to 45% (curve *7*) is accompanied by the formation of such a regular and perfect microrelief that it is difficult to distinguish it from the microrelief that is formed during the shrinkage of the polymer deformed above T_g (compare Figs. 24a and 32b). The striking similarity of these figures is indicative of an extraordinary similarity (or even the identity) of the mechanisms of formation of these microreliefs. At high strains, the shrinkage of a glassy polymer occurs in the same manner as the shrinkage of the polymer deformed above its T_g. The main feature of this deformation is its homogeneity. It is no wonder

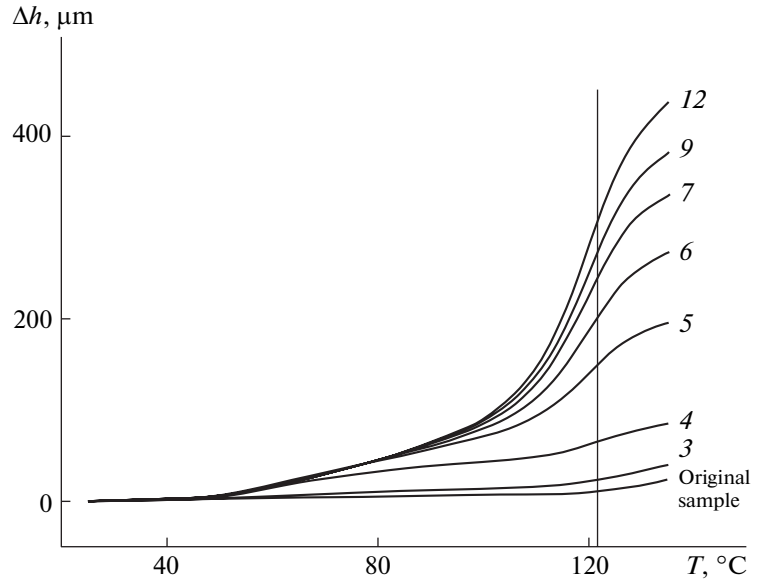

Fig. 30. Absolute variation in the height of individual PMMA layers after the deformation of a multilayer sample by 30% at room temperature. The numbers next to the curves correspond to the position of each layer with respect to the compressed surface. The vertical line denotes the glass-transition temperature of PMMA.

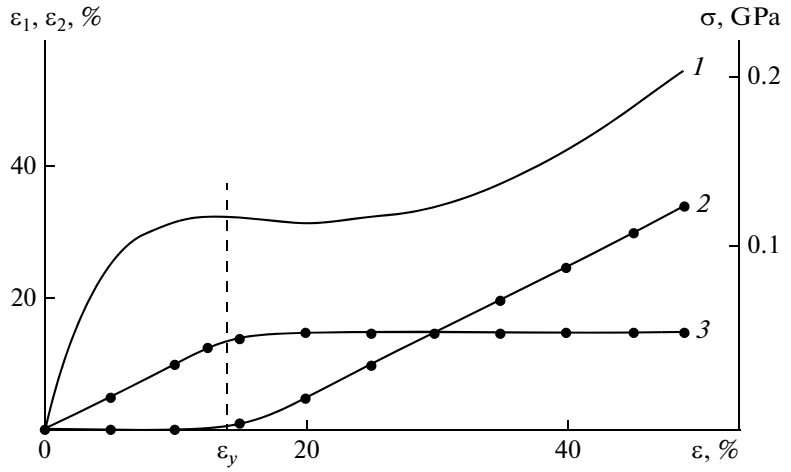

Fig. 31. (*1*) Curve of uniaxial compression of PMMA at room temperature and (*2*) the low-temperature and (*3*) high-temperature contributions to heat-induced shrinkage during annealing [66].

that the main body of the polymer participates in heat-induced shrinkage in the region of its T_g.

The used technique of the decoration of deformed polymers [11–14] suggests that the homogeneous deformation of the polymer (above and below its T_g) is accompanied by the formation of a homogeneous wavy microrelief that covers the entire surface of the polymer during its shrinkage (Fig. 24a). In the event that the deformation is inhomogeneous and occurs through the propagation of shear bands, the heat-induced shrinkage of the polymer is likewise inhomogeneous and is accompanied by the retraction of the material into the shear bands with a decrease in its surface (Fig. 24b). The effect of this retraction requires an explanation.

The structure of shear bands is very important to understanding the phenomena that occur during the inelastic deformation of glassy polymers. The shear bands that are formed in polymers are fundamentally different from the shear bands that occur in low-molecular solids. It was found [78, 79] that these bands have a complex structure. They are filled with a highly

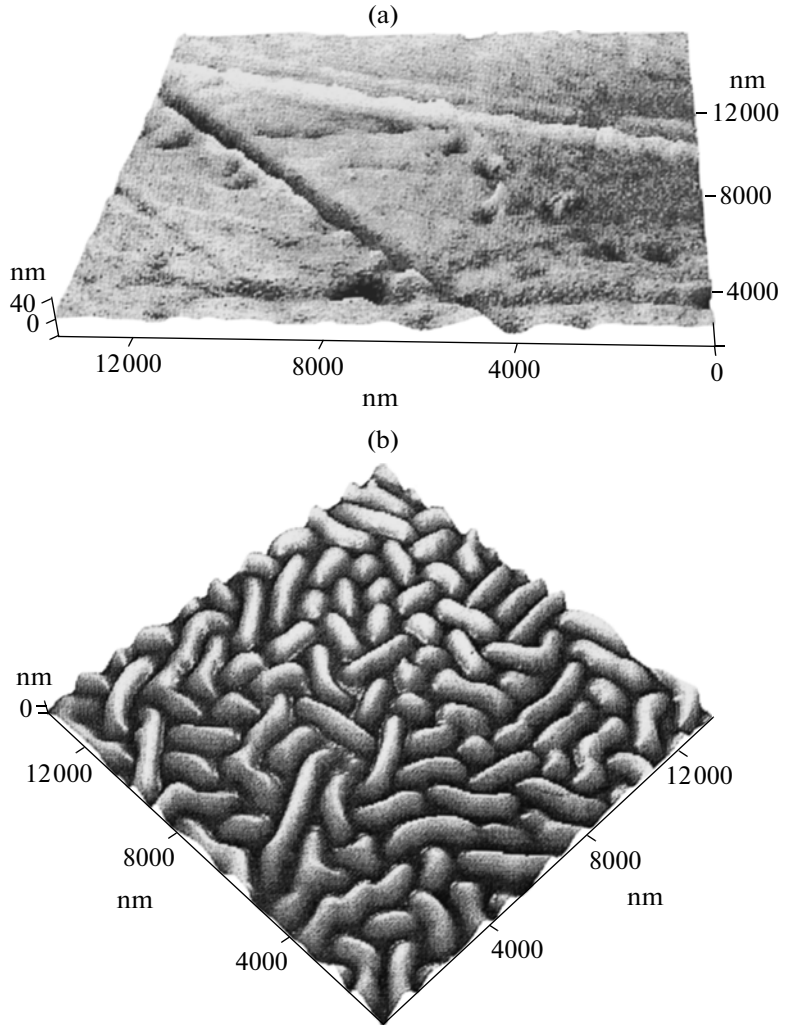

Fig. 32. AFM images of individual layers of a multilayer PMMA sample after deformation by 30%, deposition of a thin (15 nm) platinum coating on the individual layers, and annealing at 130°C. The values of shrinkage are (a) 1.7 and (b) 45%.

dispersed oriented fibrillized material that is fully analogous to the respective material that fills the volume of crazes. This important similarity is verified by direct microscopic observations. When the material that contains shear bands is subjected to minor stretching, the shear bands open to expose a crazelike structure (Fig. 33). In this case, the similarity with the structure of a craze is so striking that these open shear bands were termed "shear-band crazes" in [78].

It is very important that the diameters of fibrils in the structure of crazes and shear bands are a few nanometers [17]. This circumstance greatly affects the properties of an amorphous glassy polymer. Numerous studies have shown [80–82] that, in these thin layers (a few nanometers to a few dozen nanometers), T_g sharply decreases (by tens or hundreds of degrees). This strong decrease in T_g is caused, in particular, by the violation of the cooperativity of the glass-transition process because of the geometric constraints on the motion of polymer chains in the event that the thickness of the film or surface layer of the polymer are comparable with the unperturbed dimensions of macromolecules. The size of fibrillar entities in the structure of shear bands provides a strong decrease (by tens or even hundreds of degrees) in their T_g, a result that explains all the above features of the structural and mechanical behavior of glassy polymers from a unified viewpoint. A deformed glassy polymer is a nanocomposite that contains two fractions: the highly dispersed substance of shear bands, which has a low T_g, and an ordinary block glassy polymer, which has a T_g characteristic of a block polymer. All the previously mentioned anomalies in the properties of glassy polymers, i.e., the phenomenon of stress relaxation in a polymer in the elastic so-called Hookean region of the stress–strain curve [1], the increase in stress in a deformed glassy polymer during its isometric annealing in the temperature range below T_g [59, 60], the low-temper-

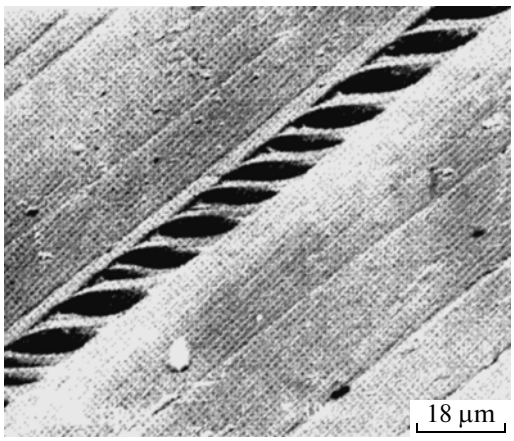

Fig. 33. Scanning electron micrograph of the fibrillar structure of a shear band in PS [78].

ature shrinkage of the deformed polymer glass in the strain range below its yield point [61], some anomalies in thermophysical properties [63, 64], and others anomalies, can be easily explained by this "two-phase" structure of the deformed polymer glass.

In addition, the highly dispersed structure of shear bands makes it possible to explain the storage of internal energy in deformed glassy polymers. An elementary calculation shows [83] that, if we assume that, at early stages (below the yield point and in the yield region), the deformation of a polymer occurs through the nucleation and propagation of shear bands with a highly dispersed fibrillar structure, the value of stored surface energy quantitatively coincides with estimates of the internal energy that is not converted to heat during the deformation of the polymer.

A comprehensive study of the structural rearrangements of the polymer conducted with the use of the method of visualization [11–14] makes it possible to propose the following pattern of inelastic deformation and heat-induced shrinkage. The deformation of a glassy polymer at early stages (below the yield point and in the yield region) results in a structure composed of two interrelated components: a portion of the oriented polymer localized in shear bands and blocks of the undeformed polymer located between them. Shear bands in polymers have a highly dispersed fibrillar structure. Consequently, their propagation is basically the introduction of a significant number of interfaces responsible for the storage of internal energy into the bulk of the polymer. This portion of the deformed polymer will be called the surface component of its structure. Recall that T_g of the polymer depends on its phase size. A fibrillized polymer localized in shear bands has a diameter of fibrillar aggregates of 1–10 nm. Therefore, this material has a lower value of T_g than that of a block polymer.

As noted above, at early stages, the polymer located between the shear bands is undeformed and its structure and properties do not differ from the original unoriented polymer. A further inelastic deformation of the polymer (the plateau region in the strain–stress curves) leads to the molecular orientation of polymer blocks located between the shear bands. The orientation of this portion of the polymer occurs without the formation of new interfaces; therefore, the storage of internal energy is hardly observed at this stage of deformation. This portion of the oriented polymer will be called the bulk component of its structure. The shear bands formed at early stages of deformation of the polymer are incorporated into the structure of the polymer and, even after its complete transition into an oriented state, preserve their identity and properties.

The annealing of the two-component system that is formed during the inelastic deformation of a glassy polymer is accompanied by the following structural rearrangements. The heating of the deformed polymer in the temperature range below its T_g causes a shrinkage of the material in the shear bands (surface component), which has a lower T_g than that of a block in a wide temperature range (the low-temperature contribution to heat-induced recovery). As a physical phenomenon, this part of the heat-induced shrinkage of the deformed polymer not only is attributed to the entropic contraction of the oriented material that fills the shear bands and has a low T_g but also is accompanied by the healing of phase boundaries in the structure of the shear bands and the relaxation of the stored internal energy.

F further heating of the polymer leads to the relaxation of the majority of the oriented polymer (the bulk component), which basically does not differ from the shrinkage of a block rubbery polymer and therefore occurs in the range of its T_g (the high-temperature contribution to heat-induced recovery).

Thus, the use of the direct microscopic technique for the visualization of structural rearrangements makes it possible to obtain new information on the deformation mechanism of amorphous polymers. This technique can be used to study both amorphous polymers in the rubbery state and the glassy state and crystalline polymers [84].

ACKNOWLEDGMENTS

We thank E.F. Oleinik for fruitful discussions.

REFERENCES

1. Yu. S. Lazurkin, Doctoral Dissertation in Mathematics and Physics (Inst. of Physical Problems, Moscow, 1954).
2. V. E. Gul' and V. N. Kuleznev, *The Structure and Mechanical Properties of Polymers* (Khimiya, Moscow, 1972) [in Russian].

3. A. A. Askadskii, *Deformation of Polymers* (Khimiya, Moscow, 1973) [in Russian].
4. J. D. Ferry, *Viscoelastic Properties of Polymers* (Wiley, New York, 1961; Mir, Moscow, 1963).
5. I. Narisawa, *Strength of Polymer Materials* (OHMSHA, 1982; Khimiya, Moscow, 1987).
6. G. M. Bartenev and S. Ya. Frenkel', *Polymer Physics* (Khimiya, Leningrad, 1990) [in Russian].
7. L. Treloar, *The Physics of Rubber Elasticity* (Oxford Univ. Press, Oxford, 1949; Inostrannaya Literatura, Moscow, 1953).
8. A. L. Volynskii and N. F. Bakeev, Polymer Science, Ser. A **51**, @ (2009) [Vysokomol. Soedin., Ser. A **51**, 1783 (2009)].
9. Yu. V. Goryunov, N. V. Pertsov, and B. D. Summ, *The Rehbinder Effect* (Nauka, Moscow, 1966) [in Russian].
10. A. L. Volynskii and N. F. Bakeev, *Solvent Crazing of Polymers* (Elsevier, Amsterdam, 1995).
11. A. L. Volynskii, A. S. Kechek'yan, T. E. Grokhovskaya, et al., Polymer Science, Ser. A **44**, @ (2002) [Vysokomol. Soedin., Ser. A **44**, 615 (2002)].
12. A. L. Volynskii, T. E. Grokhovskaya, A. S. Kechek'yan, et al., Dokl. Akad. Nauk **374**, 644 (2000).
13. A. L. Volynskii, T. E. Grokhovskaya, A. S. Kechek'yan, and N. F. Bakeev, Polymer Science, Ser. A **45**, @ (2003) [Vysokomol. Soedin., Ser. A **45**, 449 (2003)].
14. A. L. Volynskii, T. E. Grokhovskaya, V. V. Lyulevich, et al., Polymer Science, Ser. A **46**, @ (2004) [Vysokomol. Soedin., Ser. A **46**, 247 (2004)].
15. A. L. Volynskii, S. L. Bazhenov, and N. F. Bakeev, Ross. Khim. Zh. **42** (3), 57 (1998).
16. A. L. Volynskii, S. L. Bazhenov, O. V. Lebedeva, and N. F. Bakeev, J. Mater. Sci. **35**, 547 (2000).
17. A. L. Volynskii, S. L. Bazhenov, O. V. Lebedeva, et al., J. Appl. Polym. Sci. **72**, 1267 (1999).
18. S. L. Bazhenov, A. L. Volynskii, V. M. Alexandrov, and N. F. Bakeev, J. Polym. Sci., Part B: Polym. Phys. **40**, 10 (2002).
19. A. L. Volynskii, E. E. Voronina, O. V. Lebedeva, et al., Polymer Science, Ser. A **41**, @ (1999) [Vysokomol. Soedin., Ser. A **41**, 1435 (1999)].
20. A. L. Volynskii, Nauka Ross., No. 3, 4 (2002).
21. A. L. Volynskii, T. E. Grokhovskaya, A. V. Bol'shakova, et al., Polymer Science, Ser. A **46**, @ (2004) [Vysokomol. Soedin., Ser. A **46**, 1332 (2004)].
22. A. L. Volynskii, E. E. Voronina, O. V. Lebedeva, et al., Polymer Science, Ser. A **41**, @ (1999) [Vysokomol. Soedin., Ser. A **41**, 1627 (1999)].
23. Yu. K. Godovskii, in *Encyclopedia of Polymers* (Sovetskaya Entsiklopediya, Moscow, 1972), Vol. 1 [in Russian].
24. A. L. Volynskii, T. E. Grokhovskaya, A. V. Bol'shakova, et al., Polymer Science, Ser. A **48**, @ (2006) [Vysokomol. Soedin., Ser. A **48**, 2144 (2006)].
25. N. Bowden, S. Brittain, A. G. Evans, et al., Nature (London) **393**, 146 (1998).
26. W. T. S. Huck, N. Bowden, P. Onck, et al., Langmuir **16**, 3497 (2000).
27. A. L. Volynskii, T. E. Grokhovskaya, R. Kh. Sembaeva, et al., Dokl. Akad. Nauk **363**, 500 (1998).
28. A. L. Volynskii, T. E. Grokhovskaya, R. Kh. Sembaeva, et al., Polymer Science, Ser. A **43**, @ (2001) [Vysokomol. Soedin., Ser. A **43**, 239 (2001).
29. A. L. Volynskii, T. E. Grokhovskaya, R. Kh. Sembaeva, et al., Polymer Science, Ser. A **43**, @ (2001) [Vysokomol. Soedin., Ser. A **43**, 1008 (2001)].
30. A. L. Volynskii and N. F. Bakeev, *Structural Self-Organization of Amorphous Polymers* (Fizmatlit, Moscow, 2005) [in Russian].
31. V. V. Guzeev, in *Encyclopedia of Polymers* (Sovetskaya Entsiklopediya, Moscow, 1974), Vol. 2 [in Russian].
32. B. Erman, J. Polym. Sci., Part B: Polym. Phys. **21**, 893 (1983).
33. Y. S. Lipatov, A. B. Mullers, V. Privalko, and H. Sinder, Angew. Macromol. Chem. **82**, 79 (1979).
34. A. A. Dontsov, *Processes of Elastomer Structurization* (Khimiya, Moscow, 1978) [in Russian].
35. K. Dusek and W. Prins, Adv. Polym. Sci. **6**, 1 (1969).
36. B. A. Dogadkin, A. A. Dontsov, and V. A. Shershnev, *Chemistry of Elastomers* (Khimiya, Moscow, 1981) [in Russian].
37. A. J. Medalia, J. Polym. Sci. **6**, 423 (1951).
38. P. W. Allen and G. M. Bristow, J. Appl. Polym. Sci. **5**, 510 (1961).
39. N. K. Baramboim, *Mechanochemistry of High Polymers* (Khimiya, Moscow, 1982) [in Russian].
40. E. V. Reztsova and T. V. Chubarova, Vysokomol. Soedin. **7**, 1335 (1965).
41. A. Casale and R. S. Porter, *Polymer Stress Reactions* (Academic, New York, 1979; Khimiya, Leningrad, 1983).
42. L. Gonzales, A. Rodriges, A. Del Campo, and A. Marcos-Fernandes, Polym. Int. **53**, 1426 (2004).
43. A. L. Volynskii, T. E. Grokhovskaya, O. V. Lebedeva, and N. F. Bakeev, Polymer Science, Ser. A **48**, @ (2006) [Vysokomol. Soedin., Ser. A **48**, 834 (2006)].
44. D. S. Ruy, T. Inoe, and K. Osaki, Polymer **39**, 2515 (1998).
45. A. Mahendrasingam, C. Martin, W. Fuller, D. H. MacKerron, C. Rickel, and P. Engstrom, Polymer **40**, 5553 (1999).
46. A. L. Volynskii, T. E. Grokhovskaya, V. I. Gerasimov, and N. F. Bakeev, Vysokomol. Soedin., Ser. A **28**, 201 (1976).
47. A. L. Volynskii, A. G. Aleskerov, T. E. Grokhovskaya, and N. F. Bakeev, Vysokomol. Soedin., Ser. A **28**, 2114 (1976).
48. J. R. C. Pereira and R. S. Porter, Polymer **25**, 877 (1984).
49. H. J. Oswald, E. A. Turi, P. J. Harge, and Y. P. Khanna, J. Macromol. Sci., Phys. **13**, 231 (1977).
50. E. Liska, Kolloid Z. Z. Polym. **251**, 1028 (1973).
51. Jung Yul Lim and Sang Yong Kim, J. Polym. Sci., Part B: Polym. Phys. **39**, 964 (2001).
52. P. B. Bowden and S. Raha, Philos. Mag. **22**, 463 (1970).
53. A. L. Volynskii, T. E. Grokhovskaya, and N. F. Bakeev, Dokl. Akad. Nauk **400**, 1 (2005).
54. A. L. Volynskii, T. E. Grokhovskaya, and N. F. Bakeev, Polymer Science, Ser. A **47**, @ (2005) [Vysokomol. Soedin., Ser. A **47**, 540 (2005)].

55. P. B. Bowden, Philos. Mag. **22**, 455 (1970).
56. L. J. Broutman and S. M. Krishnacumar, Polym. Eng. Sci. **14**, 249 (1974).
2 57. L. Xie, D. W. Gidley, H. A. Hristov, and A. F. Yee, J. Polym. Sci., Part B: Polym. Phys. **33**, 77 (1995).
58. A. L. Volynskii, T. E. Grokhovskaya, A. V. Bol'shakova, et al., Polymer Science, Ser. A **49**, 816 (2007) [Vysokomol. Soedin., Ser. A **49**, 1946 (2007)].
59. L. A. Laius and E. V. Kuvshinskii, Vysokomol. Soedin. **6**, 52 (1964).
60. V. I. Shoshina, G. V. Nikonovich, and Yu. T. Tashpulatov, *Isometric Method of Polymer Materials Investigation* (Fan, Tashkent, 1989) [in Russian].
61. S. A. Arzhakov, Doctoral Dissertation in Chemistry (Karpov Inst. of Physical Chemistry, Moscow, 1975).
2 62. E. F. Oleinik, in *High Performance Polymers*, Ed. by E. Baer and S. Moet (Hanser, Berlin, 1991), p. 79.
63. V. A. Bershtein and V. M. Egorov, *Differential Scanning Calorimetry in Physical Chemistry of Polymers* (Khimiya, Leningrad, 1990) [in Russian].
64. J. B. Park and D. R. Uhlman, J. Appl. Phys. **44**, 201 (1973).
65. Shu-Sing Chang, J. Chem. Thermodyn. **9**, 189 (1977).
66. *Structural and Mechanical Behavior of Glassy Polymers*, Ed. by M. S. Arzhakov, S. A. Arzhakov, and G. E. Zaikov (Nova Science Commack, New York, 1997).
67. S. A. Arzhakov and V. A. Kabanov, Vysokomol. Soedin., Ser. B **13**, 318 (1971).
2 68. S. A. Arzhakov, N. F. Bakeev, and V. A. Kabanov, Vysokomol. Soedin., Ser. A **15**, 1154 (1973).
2 69. E. F. Oleinik, O. B. Salamatina, S. N. Rudnev, and S. V. Shenogin, Polymer Science, Ser. A **35**, @ (1993) [Vysokomol. Soedin., Ser. A **35**, 1819 (1993)].
70. S. V. Shenogin, G. W. H. Hohne, O. B. Salamatina, et al., Polymer Science, Ser. A **46**, 21 (2004) [Vysokomol. Soedin., Ser. A **46**, 30 (2004)].
71. T. E. Brady and G. S. Y. Yeh, J. Macromol. Sci., Phys. **9**, 659 (1974).
72. V. A. Bershtein, N. N. Peschanskaya, J. L. Halary, and L. Monnerie, Polymer **40**, 6687 (1999).
73. J. Parisot, O. Raf, and W. J. Choi, Polym. Eng. Sci. **24**, 886 (1984).
74. D. S. Sanditov and S. Sh. Sangadiev, Polymer Science, Ser. A **41**, 643 (1999) [Vysokomol. Soedin., Ser. A **41**, 977 (1999)].
75. G. P. Andrianova and V. A. Kargin, Vysokomol. Soedin., Ser. A **12**, 3 (1970).
76. Yu. S. Nadezhin, A. V. Sidorovich, and B. A. Asherov, Vysokomol. Soedin., Ser. A **28**, 2626 (1986).
77. A. S. Kechek'yan, Vysokomol. Soedin., Ser. B **29**, 804 (1987).
78. J. C. M. Li, Polym. Eng. Sci. **24**, 750 (1984).
79. K. Friedrich, Adv. Polym. Sci. **52–53**, 266 (1983).
80. J. A. Forrest and K. Dalnoki-Veress, Adv. Colloid Int. Sci. **94**, 167 (2001).
81. J. A. Forrest, Eur. Phys. J. E **8**, 261 (2002).
82. A. L. Volynskii and N. F. Bakeev, Polymer Science, 2 Ser. B **45**, 195 (2003) [Vysokomol. Soedin., Ser. B **45**, 1209 (2003)].
83. A. L. Volynskii, A. V. Efimov, T. E. Grokhovskaya, et al., Polymer Science, Ser. A **46**, 708 (2004) [Vysokomol. Soedin., Ser. A **46**, 1158 (2004)].
84. A. L. Volynskii, T. E. Grokhovskaya, A. I. Kulebyakina, et al., Polymer Science, Ser. A **51**, 396(2009) [Vysokomol. Soedin., Ser. A **51**, 598 (2009)].

SPELL: 1. affine, 2. F